Modules in the Brainstem and Spinal Cord Underlying Motor Behaviors

by
Jinsook Roh

B.A. Physics
Ewha Womans University, 2000

Submitted to the Department of Brain and Cognitive Sciences
in partial fulfillment of the requirements for the degree of

Doctor of Philosophy in Neuroscience
at the
MASSACHUSETTS INSTITUTE OF TECHNOLOGY
June, 2008

Signature of Author . . . . . .
Department of Brain and Cognitive Sciences
April 24th, 2008

Certified by . . . . . .
Emilio Bizzi, M.D.
Institute Professor
Thesis Supervisor

Accepted by . . . . . .
Matthew Wilson, Ph.D.
Professor of Neurobiology
Chairman, Committee for Graduate Studies

Modules in the Brainstem and Spinal Cord Underlying Motor Behaviors

by

Jinsook Roh

Submitted to the Department of Brain and Cognitive Sciences
on April 24, 2008
in Partial Fulfillment of the Requirements
for the Degree of Doctor of Philosophy in Neuroscience

ABSTRACT

Previous studies using reduced or intact animal preparations suggested that coordinated movements can be generated by appropriate combinations of muscle synergies controlled by the nervous system. However, which areas of the central nervous system are responsible for structuring and combining muscle synergies remains an open question. In my thesis, I have addressed the question whether the brainstem and spinal cord are involved in structuring and combining muscle synergies in order to execute a range of natural movements. The strategy to investigate this question was to analyze the electromyogram (EMG) data recorded from the leg muscles during frog motor behaviors before and after neuronal transection. In my two sets of experiments, EMGs were recorded before and after transection at the level of the caudal end of the third ventricle and at the level of the caudal end of the pons in two groups of frogs. When the section was at the level of rostral midbrain, movements such as jumps, swims, kicks, and walks could be performed by the animals. In contrast, when the transection was at the level of rostral medulla, only a partial repertoire of natural movements could be evoked. Systematic analysis of muscle synergies in these preparations found two different types of synergies: (1) synergies shared by intact animals and animals with transection, and (2) synergies specific to individual motor behaviors. In addition, almost all synergies utilized in the execution of natural motor behaviors remain invariant after transection at the level of the caudal end of the third ventricle or at the level of the caudal end of the pons. The results suggest the following: (1) the neural network within the brainstem and spinal cord are necessary and sufficient in combining muscle synergies in the organization of natural movements, and (2) the neural circuitries within the medulla and spinal cord are sufficient to structure the repertoire of muscle synergies in natural motor behaviors. Overall, the major findings of this study indicate how the neural divisions in the CNS are functionally differentiated for structuring and combining modules in execution of natural movements.

Thesis Supervisor: Emilio Bizzi, M.D.
Title: Institute Professor, MIT

Acknowledgments

Simply, I am grateful to God for all people, experiences, and the promises He provided me in my life at MIT.

Emilio Bizzi, Chris Moore, Sebastian Seung, Michale Fee, Ann Graybiel, Martha Constantine-Paton, Peter Schiller, Gerald Schneider, Margo Cantor, Charlotte Potak, Caterina Stamoulis, Vincent Cheung, Matt Tresch, Simon Overduin, Andrea d'Avella, Philippe Saltiel, Robert Ajemian, Andrew Richardson, Chris Bae, Maureen Holden, Max Bernike, Alessandro d'Ausilio, Timothee Doutriaux, Glenda Lassi-Tucci, Silvestro Micera, Tommaso Borghi, Farah Zaheer, Jeffrey Moore, Terra Barnes, Show Ming Kwok, Emily Hueske, David Nguyen, Yuri Ostrovsky, Neville Sanjana, Rebecca Schwarzlose, Nathan Wilson, Jiyeon Choi, Eunkyoung Kang, Youngsook Jung, Daeman Lee, Seungeun Oh, Yoonji Lee, Taewhan Kim, Daesung Choi, Hanpil Lee, David Choi, Kyesook Park, Amy Oh, Hang Lee, Soochan Bae, Eunkyung Koh, Wonjoo Jeong, Byunggook Kwon, friends in the Three-fold prayer meeting at MIT, friends at MIT, friends in First Korean Church in Cambridge, and my family …

All my achievements and failures, in faith and science, which made me even stronger and wiser than before …

Trust in the LORD with all your heart and lean not on your own understanding; in all your ways acknowledge him, and he will make your paths straight. –Proverbs 3:5-6

I will put my Spirit in you and you will live, and I will settle you in your own land. Then you will know that I the LORD have spoken, and I have done it, declares the LORD. –Ezekiel 37:14

Contents 7

List of figures

List of tables

Chapter 1

Introduction

One of the fundamental challenges in neuroscience is to understand how the nervous system orchestrates motor acts and movements. The brain may control complex movements through flexible combination of motor primitives, where each primitive is an element of computation in the sensorimotor map that transforms desired limb trajectories into motor commands (Thoroughman and Shadmehr, 2000). This thesis addresses the degree to which the brainstem and spinal cord are involved in structuring and combining motor primitives underlying natural motor behaviors.

A challenge and a potential strategy of the nervous system in movement execution: redundancy in specifying movement trajectories and modular organization

The central nervous system specifies the motor commands required to generate purposeful, well-coordinated movement in the workspace. The difficulty in specifying muscle activations for movement execution lies in the fact that multiple combinations of muscle activation patterns can result in the same movement trajectory.

Bernstein (1967) was one of the first to address the issue of the large number of degrees of freedom in the musculoskeletal system and their coordination in the motor systems. Due to anatomical, mechanical, and physiological sources of indeterminacy, movements are not completely determined by effector processes (Bernstein, 1976). For example, the torque generated by a muscle depends on the configuration of the limb (anatomical indeterminacy). A source of mechanical indeterminacy is the fact that movement is determined by the forces only when the initial conditions, positions, and velocities are specified. These examples demonstrate that the relationship between muscle activation patterns and performed movement is context-dependent, which increases the difficulty to specify muscle activation for producing purposeful movement. In addition, given that different combinations of muscle activation result in the same trajectory, the CNS-controlled musculoskeletal system is a redundant system.

A potential strategy for resolving the redundancy is that, during motor execution, multiple muscles are activated together as a fixed group, or as a muscle synergy, and the final motor patterns emerge from an organized combination of the activations of a small number of synergies, each potentially comprising different or same muscles (Greene, 1972; Kugler et al., 1980; Lee, 1984; Macpherson, 1991).

Generating muscle patterns through a set of muscle synergies simplifies control, at least theoretically, in several different ways (Cheung, 2007). First, the synergies reduce redundancy by constraining the set of all conceivable muscle patterns (Bernstein, 1967; Full and Koditschek, 1999). Second, by constraining a group of muscles to act as a unit, a synergy may serve to eliminate certain muscle patterns that lead to uncoordinated movements (Tuller et al., 1982). Also, if each muscle synergy is composed in such a way that co-activations of the synergy's constituents always result in the execution of certain simple biomechanical functions, or movements with certain predictable features, then motor commands may be generated easily through specifications of the synergies' activation level without the need to explicitly solve the inverse dynamics equations. Finally, as a result of being structured to perform some simple biomechanical or kinematic functions, muscle synergies may also facilitate the generalization of motor control (Poggio and Bizzi, 2004), in the sense that altering the activations of the same set of synergies might enable the animal to perform the same behavior in a very different dynamical environment (Mussa-Ivaldi, 1997), or a different behavior in the same environment (d'Avella et al., 2003).

Evidence for modular organization of the spinal cord

There have been a variety of data that support the spinal encoding of motor modules in a range of animals. Brown (1911) first proposed 'half-center' model as a central mechanism for the alternation of flexion and extension. In the model, each half-center was suggested to activate either flexors or extensors, and the two half-centers were thought to be coupled by reciprocal inhibition. Later, Lundberg, Jankowska, and collaborators identified two spinal networks, activated by the 'flexor reflex afferents' or FRA, capable of generating an alternating activity in flexor and extensor motoneurons. They proposed that the central mechanism capable of generating the locomotor pattern, or central pattern generator (CPG), could be implemented by these two networks (Jankowska et al., 1967a, b; Engberg and lundberg, 1969).

Grillner (1981) proposed an alternative view that spinal motor networks corresponding to limb CPGs could be divided into and be composed of several 'unit burst generators', which can be recruited into a reciprocally organized common network (Grillner, 1981). This modular architecture is more flexible than the half-center model in the sense that it could

also explain different patterns of movements simply by changing the coupling between different generators. For example, in the lamprey study, Grillner and collaborators have shown the existence of spinal modules, repeated every two or three spinal sebments, that can generate the alternating burst activity necessary for swimming (Grillner et al., 1995). During swimming, the different segments are coordinated by a constant phase delay. Most interestingly, by changing the lag between adjacent modules, the spinal network can flexibly generate forward (positive rostro-caudal lag) or backward (negative lag) swimming. The circuitry of a spinal module has been reconstructed in the frog tadpole (Roberts et al., 1998) as well.

In the turtle, Stein and collaborators have assessed the organization of the spinal circuitry in controlling hindlimb scratching. Depending on the location of a cutaneous stimulus, the spinal turtle can generate three different forms of scratching (rostral, pocket, and caudal) (Mortin et al., 1985). The muscle patterns show a similar alternation of activity in hip protractors and retractors across the three forms but a distinctive timing of knee extensors relative to the hip cycle (Robertson et al., 1985). These patterns are generated by a CPG in the spinal cord that appears to be organized in ipsilateral and contraleteral flexor and extensor modules (Stein et al., 1995). Each module contains motonuerons for synergistic muscles at one joint, excitatory interneurons that project to the motoneurons and to agonist modules, and inhibitory interneurons that project to antagonist modules. The separate burst-generators in the spinal cord for forelimb flexion and extension during walking have been identified in the mudpuppy as well (Cheng et al., 1998).

Spinalized or intact frogs have been used in a series of experiments in order to address the issue of modularity in the spinal cord. Bizzi and his colleagues found that only a few stereotypical force fields could be evoked by repetitive microstimulation in the spinal cord consistently across different spinalized frogs (Bizzi et al., 1991; Giszter and Kargo, 2000). Simultaneous stimulation at two different spinal sites resulted in a force field that was a simple combination of the two separate fields produced by stimulating each site separately (Bizzi et al., 1991). These results led to suggest that complex movements may be produced by the flexible linear combination of a small number of motor primitives, later called "muscle synergies" (Tresch et al., 2002). In rats, the stimulation experiments were repeated to test the existence of motor building blocks in mammals (Tresch and Bizzi, 1999). In addition, focal intraspinal NMDA iontophoresis that evoked activation of local interneurons in the

frog spinal cord (Saltiel et al., 1998; Saltiel et al., 2001; Saltiel et al., 2005) demonstrated evidence of existence of spinal modules topographically organized as patchy structures in the lumbar spinal cord region. The study of spinal wipe reflexes showed that the wipe reflex in spinal frogs can be constructed as the appropriate time-varying summation of the force field primitives found with electrical stimulation, supporting the idea of modular organization in the spinal circuitry (Giszter et al., 1993; Kargo and Giszter, 2000a; Kargo and Giszter, 2000b). In intact frogs (d'Avella et al., 2003; d'Avella and Bizzi, 2005), decomposition of muscle activations as combinations of synchronous or time-varying muscle synergies demonstrated how the muscle patterns are spatially organized or what specific characteristics the muscle activation waveforms have.

However, there have been no studies that demonstrate whether the motor modules observed in a range of natural movements are encoded by the spinal cord and its heavily connected neural circuitries. This was the direct motivation of the current thesis to assess the extent of modulation of muscle synergies observed in brainstem and medullary preparations from the supra-brainstem and supra-medullary networks, respectively.

Evidence for neural encoding of muscle synergies

The increasing amount of experimental evidence has led to the idea that motor commands and movements in both vertebrates and invertebrates are generated by combination of a small number of elementary building blocks, muscle synergies. These experimental results have been acquired from a variety of intact or reduced animal preparations including the turtle, mudpuppy, frog, and mammal (Fetz et al., 2000; Tresch et al., 2002; Miller, 2004; Bizzi et al., 2007). The modules, building blocks of motor command, have been investigated at several different levels, for instance, at the neural, dynamic, and kinematic levels (Flash and Hochner, 2005). The behaviors analyzed range from simple frog reflexes (Bizzi et al., 1991) to complex primate hand grasping (Miller, 2004; Overduin et al., 2008). The following studies have addressed the modular organization of movements.

To search for muscle synergies, Tresch et al. (1999) applied the non-negative least-squares algorithm to EMG data recorded from nine hindlimb muscles in the spinalized bullfrog during spinal reflexes evoked by cutaneous stimulation of different regions of the skin surface of the hindlimb. The EMG model assumed time-invariant synergies (i.e., identifying

patterns of covariation among subsets of muscles at a given moment) and their structure demonstrated the spatial relationship of muscle activation (i.e., balance of amplitudes of muscle activation), while the corresponding synergy coefficient was time-varying and contained the temporal information of each behavioral episode. The results of the study showed that a combination of these synergies with different weightings can describe the observed original muscle activation patterns during the frog hindlimb withdrawal reflexes. Overall, the data led to the idea that the vertebrate spinal cord system can produce movement as a linear combination of muscle synergies.

In their study of motor responses evoked by NMDA iontophoresis, Saltiel et al. (2001) recorded EMGs from 12 hindlimb muscles in the spinalized frog. The potential advantage of the focal intraspinal NMDA microstimulation is to selectively evoke activation of local interneurons in the frog spinal cord (Saltiel et al., 1998; Saltiel et al., 2001; Saltiel et al., 2005) and to record EMGs generated by direct stimulation of spinal interneurons. In the study, the time-invariant synergy model and the non-negative least-squares algorithm were applied as in Tresch et al. (1999). The major finding was that a small number (i.e., seven) of patterns of muscle coactivation, or muscle synergies, explains a large amount of data variance, about 91%. Furthermore, the results suggested that the synergies are tophographically organized as patchy structures in the lumbar spinal cord region.

Instead of studying the motor behaviors observed in the reduced, spinalized preparations, d'Avella et al. (2003) investigated the EMGs recorded from 13 hindlimb muscles during natural movements including kicking, jumping, swimming, and walking in the intact bullfrogs. The major differences between the two previous studies (Tresch et al., 1999; Saltiel et al., 2001) and the given study are movement repertoire recorded in the experiments and the synergy model; this study decomposed natural motor behaviors, assuming that muscle synergies (not the corresponding coefficients) have temporal information of movement (i.e., time-varying synergies). The results of the work demonstrated that the EMGs recorded from 13 muscles for each motor behavior can be reconstructed by combining 5-7 muscles synergies. More interestingly, d'Avella et al. (2003, 2005) showed that there are similarities among the synergies extracted from different behaviors, supporting the idea of modular organization of natural movement.

Hart and Giszter (2004) recorded EMGs from 10 hindlimb muscles of the bullfrog in brainstem animals (i.e., animals after transection at the level of the caudal end of the pons)

during brainstem behaviors, which include kicks, jumps, some spontaneous locomotion, and complex escape sequences, and in spinal preparations during spinal reflexes. The motor building blocks were extracted using independent component analysis; the original EMG dataset was modeled as a combination of "unit bursts," equivalent to muscle synergies, and "premotor drives," time-varying activation coefficients of the model. The data demonstrated that brainstem and spinal motor primitives are similar in the sense that there are six common drives and ~275 ms dominant duration of bursts. However, the results showed major differences in two sets of synergies, e.g., brainstem frogs have more regular bursts of smaller amplitude. The study suggested that richer behaviors of brainstem frogs seem to be the result of altered synergies with more "focused" muscle activation and that descending pathways may take part in fine-tuning the modular organization of drives seen in the isolated spinal cord.

The results of studies described above suggest a strategy of the CNS for generating motor command with efficiency and ease in combining a small number of muscle synergies. However, the precise role of sensory feedback in organizing the modules was an open question. Cheung et al. (2005) recorded EMGs from 13 hindlimb muscles of the frog during jumping and swimming, before and after deafferentation. The results demonstrated that most muscle synergies underlying natural jumps and swims remain constant, in terms of the muscle subspace spanned by the sets of synergies underlying motor outputs, after removing sensory information into the CNS from the periphery by severing dorsal roots. The results support the idea, the neural encoding of muscle synergies, by demonstrating that most of the muscle synergies underling locomotory behaviors are centrally organized and that the role of sensory feedback is to modulate activation of the centrally organized synergies, not to change the structure of synergies.

Muscle synergies have been observed by EMG analysis in other animal preparations and behaviors as well. The studies include postural responses in the cat (Ting and Macpherson, 2005; Torres-Oviedo et al., 2006; Lockhart and Ting, 2007; McKay and Ting, 2007), locomotion in the cat (Krouchev et al., 2006), grasping and reaching in the monkey (Overduin, 2006), human hand postures (Weiss and Flanders, 2004), human postural responses (Krishnamoorthy et al., 2003; Torres-Oviedo and Ting, 2007), human locomotion (Cappellini et al., 2006; Ivanenko et al., 2007), and human arm movement (Sabatini, 2002; d'Avella et al., 2006).

The brainstem and spinal cord: candidate neural divisions to structure and combine muscle synergies

Locomotor behaviors such as swimming and walking involve the activation of many muscles. CPGs controlling locomotion are localized in the spinal cord, and activity in the CPG is turned on and maintained by inputs from descending locomotor commands originating from neurons in the brainstem (Kiehn, 2006). Thus, understanding the anatomical connectivity between the spinal cord and brainstem is critical to understanding of the control of movement organized in a modular fashion, the major topic of the current thesis.

i) Ascending spinal pathways and descending supraspinal fibers

In anterograde degeneration studies (Ebbesson, 1969, 1976) of the bullfrog, two systems of ascending spinal projections have been found: (a) a primary afferent ascending spinal projection via the dorsal funiculus to the dorsal column nucleus, and (b) a secondary afferent projection via the lateral funiculus, i.e., the spinal lemniscus, to the reticular formation, the mesencephalon, and possibly to the thalamus. In addition, there is evidence for the presence of an anuran homologue of the mammalian spinocervicothalamic system (Munoz et al., 1996).

In anurans, the descending supraspinal system from the brainstem to the spinal cord is well developed. The rhombencephalic reticular formation, a part of the brainstem, is the main target for afferents from the spinal cord. The reticulospinal, interstitiospinal, and vestribulospinal fiber systems descend from the brainstem to the spinal cord. Interestingly, reticulospinal fibers establish monosynaptic connections with motoneurons in the spinal cord. There has been evidence of a descending lateral funicular axon system that synapses directly upon lumbar motoneuron somata and proximal dendrites. Physiological studies in bullfrogs have shown that some of these fibers are supraspinal in origin and that they terminate upon both flexor and extensor motoneurons (Cruce, 1974b). This pathway may be especially developed to subserve the rapid burst of motorneuron activity which activates the characteristic leap of the frog. Cruce's (1974b) data suggest that the lateral funicular fibers responsible for the monosynaptic EPSPs originate in the reticular formation of the caudal rhombencephalon. In anurans, the reticular formation may represent a 'final common

supraspinal' pathway by way of which higher centers can influence spinal motor mechanisms (ten Donkelaar, 1982, 1990). The brain stem reticular formation plays a major role in basic function such as prey-catching, feeding behavior, and locomotion.

Lesion studies of the vestibular nuclear complex in the bullfrog (Fuller, 1974), have demonstrated a vestibulospinal tract projection bilaterally via the ventral funiculus to the spinal cord terminating in the medial region of the ventral horn, i.e., the ventromedial spinal field, but also in the medial column of motorneurons. Vestibulospinal projections have been shown to impinge monosynaptically on the lumbar spinal motoneurons innervating the hindlimb muscles (Barale et al., 1971; Magherini et al., 1974). Thus, this pathway, as well as the reticulospinal fiber system, may be especially designed to underlie the rapid burst of motoneuron activity, which activates the rapid movement of the frog.

In addition, distinct contralateral tectospinal projection to the medial part of the ventral horn of the cervical intumescence was found in Rana pipiens (Rubinson, 1968), but telencephalospinal projections are absent (Nieuwenhuys and Opdam, 1976). Thus, overall, the spinal cord has sophisticated anatomical connection to the brainstem and other supraspinal systems via ascending and descending projections.

ii) Anatomical substrates that can evoke pattern of simultaneous muscle activation

In the spinal cord, motoneurons innervating forelimb and hindlimb muscles are clustered in longitudinally arranged motor pools. The motor pool organization, monosynaptic connections of reticulospinal and propriospinal fibers, and massive dendritic trees of motoneurons in anurans may also correlate with muscle function, especially with simultaneous muscle activation.

The mediolateral position of hindlimb motor pools remarkably corresponds with the participation of muscles in the main postures of the hindlimb, i.e., squatting and kicking (Cruce, 1974a; Hulshof et al., 1987). The entire system appears to be designed to produce the characteristic sudden simultaneous extensor and flexor movements of all the joints of both hindlimbs by which anurans swim in water and jump on land. Electrically mediated crossed interactions among lumbar motoneurons may serve as a means of coordinating muscle groups of opposite sides that are used in movements that require bilateral synchronization (Erulkar and Soller, 1980).

As described above, reticulospinal fibers, vestibulospinal fibers, and also propriospinal

fibers, establish direct monosynaptic connections with lumbar motoneurons (Cruce, 1974b; Shapovalov, 1975; Barale et al., 1971; Magherini et al., 1974). Such a wide distribution of reticulospinal, vestibulospinal, (and possibly also propriospinal) fibers to the lumbar motorneuron region may well be suited for producing the simultaneous extension and flexor movements that are characteristic of anuran locomotion.

Furthermore, anuran motoneurons have massive dendritic trees (Sala y Pons, 1892; Ebesson, 1976; Szekely, 1976; Bregman and Cruce, 1980; Rosenthal and Cruce, 1985). The dorsolateral and ventromedial neurons have partly overlapping dendritic arborizations, although the lateral motoneurons appear to have more dendrites in the dorsal part of the lateral funiculus, whereas the medial motoneurons send dendrites into the contralateral ventral horn and ventral funiculus. In Rana pipiens, the dendrites of medial motoneurons in the brachial cord have a greater rostrocaudal extent than those of the lateral motoneurons (Rosenthal and Cruce, 1985).

iii) The role of the spinal cord in movement initiation and termination

In general, the initial postural adjustments of escape behavior should be executed rapidly; thus, stimulation of the lower body in spinal or intact amphibians could elicit startle responses solely through spinal initiation pathways. In addition, the locomotor component elicited by the same stimuli in most spinal animals is brief and undirected, while in intact animals this component is goal-directed and may be of long duration. Thus, the direct activation pathways from spinal input to the CPGs might activate the initial phase of locomotor responses and then provide additional excitation or biasing to spinal motor networks once supraspinal command systems have taken over (McClellan, 1986).

There have been studies on the role of the spinal cord in termination of motor behavior (Boothby and Roberts, 1992a, b). The study of the mechanisms responsible for termination of rhythmic locomotor behavior in Xenopus laevis tadpoles has shown that X. laevis embryos stop swimming in response to pressure on the cement gland (Roberts and Blight, 1975). Intracellular recordings from spinal neurons active during swimming have shown that pressure on the cement gland evokes compound, chloride-dependent inhibitory postsynaptic potentials. The stopping response depends on the excitation of pressure-sensitive trigeminal receptors which innervate the cement gland (Boothby and Roberts, 1992b). The release of excitatory amino acid excites brainstem GABAergic reticulospinal neurons, which inhibit

spinal neurons to turn off the CPG for swimming.

Goals and questions of the current thesis

The goal of this thesis is to test the hypothesis that the neural machineries within the brainstem and spinal cord structure and combine muscle synergies, or motor primitives, in order to do motor coordination for execution of natural movements. To test the given hypothesis, two different sets of experiments, each with two substages of EMG recording sessions at different times, were designed and performed. The first set of experiments tested whether the neural circuitries within the brainstem and spinal cord are sufficient to structure and combine muscle synergies underlying natural movements including jumping, swimming, kicking, and walking. The second set of experiments tested whether the entire repertoire of muscle synergies underlying the four major types of natural movements is structured by the neural circuits in the medulla and spinal cord. EMGs from 12-13 muscles of the bullfrog hindlimb during natural behaviors (jumping, swimming, kicking, and walking) were recorded as well as brainstem behaviors (i.e., behaviors observed after transection at the level of the caudal end of the third ventricle). In the other set of experiments, EMGs were recorded from 12-13 muscles of the bullfrog hindlimb during natural behaviors as well as medullary behaviors (i.e., behaviors observed after transection at the level of the caudal end of the pons). While the transection for the first set of experiments was performed to keep the brainstem and the nervous system caudal to the brainstem intact, the second form of transection aimed to keep the medulla, the spinal cord, and the connected peripheral nervous system intact.

The non-negative matrix factorization algorithm was applied to EMG data sets recorded from intact and reduced preparations to confirm the low dimensionality of the data sets. The results indicate the presence of two different types of synergies: (1) synergies common both to natural behaviors in intact animals and to the behaviors evoked in the reduced preparations (i.e., brainstem or medullary animals), and (2) synergies specific to individual motor behaviors. Four to six synergies can explain >90% of the total variance of the EMG data for all natural and brainstem movements, while six to seven synergies account for the same amount of variability in the dataset recorded from the reduced preparation when the medulla is connected to the spinal cord. Furthermore, while the brainstem preparations can

perform all major types of natural movements observed in intact animals, only a partial repertoire of natural movements can be evoked in the medullary preparations. In addition, almost all muscle synergies utilized to generate natural motor behaviors remain invariant after transection either at the level of the caudal end of the third ventricle or at the level of the caudal end of the pons. Thus, overall, the major findings of the given study suggest the following that indicate the functional differentiation of neural divisions in the execution of movement: (1) the neural circuitries in the brainstem and spinal cord are necessary and sufficient to combine muscle synergies in coordination of natural motor behaviors, and (2) the neural circuitries in the medulla and spinal cord are sufficient to structure the repertoire of muscle synergies underlying natural movements.

Chapter 2

Modules in the brainstem and the spinal cord underlying natural motor behaviors

INTRODUCTION

Many studies have supported the idea that vertebrate spinal motor systems are organized in a modular fashion. However, there have been no studies demonstrating that the modules observed in intact and reduced preparations are generated by the localized neural divisions including the spinal cord.

Thus, my thesis deals with two main questions: (1) whether the neural circuitries within the brainstem and spinal cord are necessary and sufficient to structure and combine muscle synergies in execution of natural motor behaviors, and (2) whether the neuronal machineries in the medulla and spinal cord are sufficient to structure the entire repertoire of muscle synergies explaining the four major types of natural movements.

In order to assess the two main questions listed above, I performed two sets of experiments. In the first set of experiments (the ***intact vs. brainstem*** condition), I addressed the first main question. I recorded EMG data from 12-13 muscles in the frog hindlimb during movements before and after transection at the level of the caudal end of the third ventricle. To maximize the data variability, I recorded four major types of motor behaviors such as jumps, swims, kicks, and walks before and after the transection. In the second set of experiments (the ***intact vs. medullary*** condition), I recorded the EMGs during movements before and after transection at the level of the caudal end of the pons. By applying the non-negative matrix factorization algorithm, I confirmed the low dimensionality of the data sets and searched for (1) synergies shared by natural movements and movements observed in "brainstem" animals (i.e., animals with transection at the level of rostral midbrain) or "medullary" animals (i.e., animals with transection at the level of rostral medulla), and (2) synergies specific to the individual behaviors. Furthermore, the major different between brainstem and medullary preparations is the repertoire of movements observed in the preparations. The brainstem preparations, but not medullary preparations, can perform the entire repertoire of four major motor behaviors, suggesting that the brainstem and spinal cord are involved in combining muscle synergies in the execution of the natural movements. In addition, almost all synergies utilized to generate natural motor behaviors remained invariant after transection either at the level of the caudal end of the third ventricle or at the level of the caudal end of the pons. The result supports the idea that the medulla and spinal cord are sufficient to structure muscle synergies underlying natural movements. Overall, the

findings of the study indicate how the neural divisions in motor coordination and movement execution are functionally differentiated.

MATERIALS AND METHODS

Surgeries

All procedures were approved by the Committee on Animal Care at MIT. Six adult bullfrogs (Rana catesbeiana, 218-396 g) were studied: three for comparing behaviors performed before and after transection at the level of the third ventricle (the ***intact vs. brainstem*** condition) and three for comparing behaviors generated before and after transection at the level of the caudal end of the pons (the ***intact vs. medullary*** condition). A "brainstem preparation" implies a frog with intact midbrain and the nervous systems caudal to the midbrain (see Figure 1*B*). Similarly, "medullary preparation" refers to an animal preparation that produces behaviors when the medulla and spinal cord are connected to the musculoskeletal system (see Figure 1*C*).

Two surgeries were performed on each frog on separate days: one for implantation of EMG electrodes and the other for transection. After the injection of 0.1 mg/g of 5% tricaine (MS-222, Sigma) into the dorsal lymph sac, the frog was placed on a pad of crushed ice and kept on ice during the two surgical procedures.

During the first surgery, in order to implant bipolar electrodes in 13 muscles, the skin was cut on the dorsal and ventral surfaces of the thigh and on the dorsal surface of the calf. The implanted hindlimb muscles were: rectus internus (RI), adductor magnus (AD), semitendinosus (ST), sartorius (SA), vastus internus (VI), rectus anterior (RA), vastus externus (VE), iliopsoas (IP), biceps femoris (BF), semimembranosus (SM), gastrocnemius (GA), tibialis anterior (TA), and peroneus (PE) (according to the nomenclature of Ecker (1971)). Most of these muscles are biarticular. RI, ST, and SM are both hip extensors and knee flexors, while AD is a hip extensor. VE, VI, and RA are both hip flexors and knee extensors. BI and SA are both hip flexors and knee flexors, while IP is a hip flexor. There are muscles connected to the knee and ankle joints: GA, TA, and PE. GA is both a knee flexor and an ankle extensor, while PE and TA are both knee extensors and ankle flexors (The sign of the moment arms around the hip, knee, and ankle joints of the muscles are based on the results of Kargo and Rome (2002) and Gonzalez (2003)). The set of muscles whose activity was recorded includes almost all of the major muscles of the frog hindlimb. Each pair of

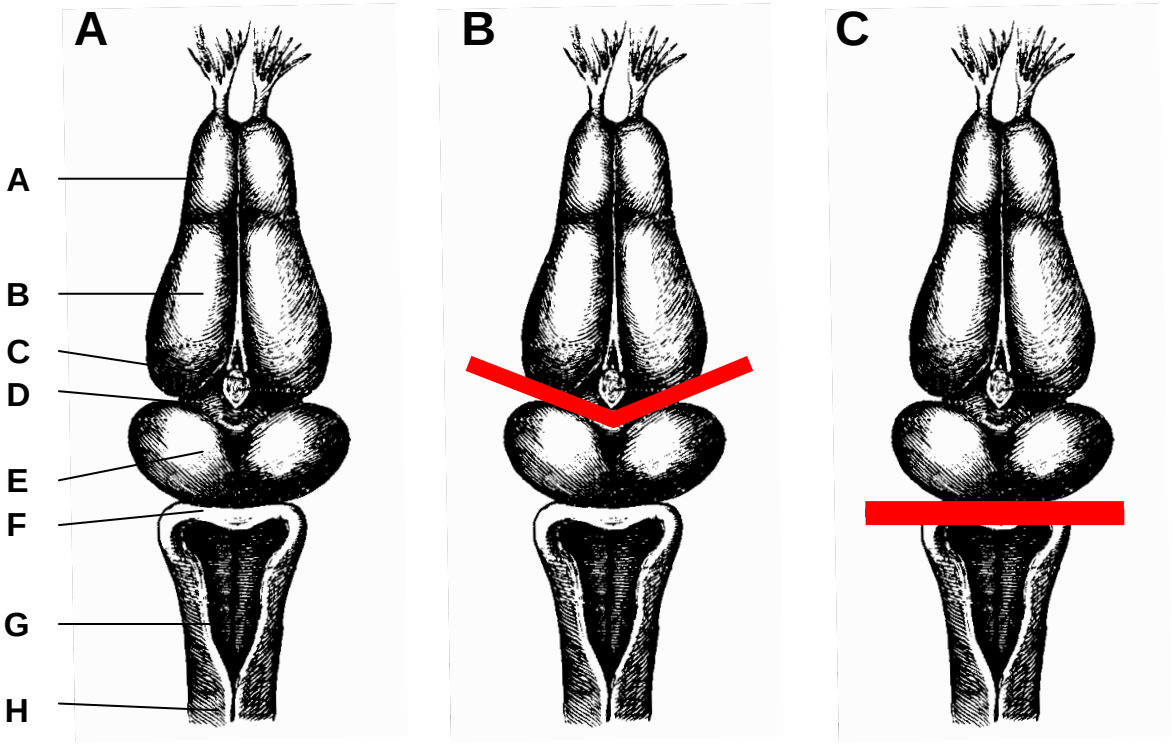

Figure 1. A schematic diagram of the bullfrog CNS. ***A***, The entire intact CNS. A, olfactory lobes; B, cerebral hemispheres; C, pineal gland; D, thalamus; E, optic lobes; F, cerebellum; G, medulla; and H, spinal cord. ***B***, In the first set of experiments to compare movements in intact and "brainstem" animals (the ***intact vs. brainstem*** condition), the transection was performed at the level (marked by red lines) of caudal end of the third ventricle to keep the entire brainstem and the neural divisions caudal to the brainstem intact. ***C***, In the second set of experiments to compare movements in intact and "medullary" animals (the ***intact vs. medullary*** condition), the transection was performed at the level (marked by a red line) of caudal end of the pons (by removing the deep cerebellar nuclei) to keep the medulla and spinal cord intact.

electrodes used consisted of multi-strained Teflon-coated stainless steel wires (A-M Systems, Inc., Calsborg, WA) that had a small wax disc, as an anchor of the implantation, in the middle of two knotted wires. The electrodes were exposed by 2 mm, and 2-3 mm apart from the disc. After the implantation on the muscles, the wires were guided subcutaneously to the back through a skin incision on the back. At the end of the implantation, all 13 pairs of wires from 13 different muscles were connected to a 37-pin miniature connector, and secured to the back skin with a custom-made plastic platform and Nexaband glue (Verterinary Products Laboratories, Phoenix, AZ). The crimp contacts were insulated by both epoxy and dental wax for increasing mechanical stability. The pinned D-sub connector was connected to the data acquisition system (DataWave) to record electromyography (EMG). Movements were not impaired by the pinned connector, and the frogs appeared to behave naturally.

During the second surgery, the same animal was transected at various levels, depending on the goal of the experiment to compare the ***intact vs. brainstem*** or the ***intact vs. medullary*** condition. After exposing the cervico-medullary junction, frogs were severed either at the level of the caudal end of the third ventricle or at the caudal end of the pons (removing the deep cerebellar nuclei from the animal) with fine scissors and forceps. Completeness of the transection was double-checked, and small pieces of gel foam were inserted into the place of the transection.

Experimental procedure

In order to assess the main questions of our studies, two different sets of experiments were performed: (1) the ***intact vs. brainstem*** condition and (2) the ***intact vs. medullary*** condition. During experiments of the the ***intact vs. brainstem*** and the ***intact vs. medullary*** conditions, all major types of natural behaviors of the frog and medullary behaviors were recorded.

The sequence of a set of experiments involved: implantation of EMG electrodes, recording natural behaviors, transection, and recording brainstem or medullary behaviors. Collected natural behaviors and brainstem behaviors (i.e., behaviors after transection at the level of the caudal end of the third ventricle) have same behavioral repertoires: jumps, swims, kicks, and walks. Between surgeries and experimental sessions, the frog was allowed at least 12 h for recovery from the surgery. A few episodes of jumping, swimming, kicking, and walking were spontaneous, but most of them were elicited by lightly scratching the skin of

either the hind limbs or the body trunk with a pair of sharp forceps. Episodes of both in-phase and out-of-phase swimming were either spontaneous or elicited by mildly touching the hind limbs with a plastic rod. During all swimming trials, removable light-bodied Permlastic (Kerr USA, Romulus, MI) was also used for water-proofing of the EMG-electrode D-sub connector. In order to evoke natural, brainstem, or medullary behaviors, the cutaneous stimulation was given on the ipsilateral or contralateral areas of the body including the rostral and dorsal surface of the leg, the web of the foot, toes, the caudal surface of the thigh or the region around the cloacal fold. The areas of skin were selected because the most significant EMG activities during natural, brainstem, or medullary behaviors without movement artifacts in the EMGs were acquired by stimulating those regions. All jumping, swimming, kicking, walking, and medullary trials were videotaped, and the EMG activities were recorded during all types of behavioral episodes. Video recordings were synchronized by a digital counter. After all experimental procedures, correct placement of electrodes in muscles was confirmed in postmortem examinations after all experimental procedures. Frogs were kept in a refrigerator at 9℃ between surgical procedures and between experiments.

The medullary motor behaviors included kicks, walks, and wiping behaviors. The movements were mainly evoked by mild pinching and scratching the skin of the body parts as described above, but some spontaneous locomotion was observed as well. Neither jumps nor swims were observed in animals after complete bilateral transection at the level of the caudal end of the pons. Since the number of wiping behaviors recorded was small and the behavior was not the major interest of the experiments, I only analyze the EMG data recorded during kicks and walks in medullary preparations.

Data collection and preprocessing

EMG data during all movements recorded in intact, brainstem, and medullary preparations were band-pass filtered (10 Hz to 1 kHz), amplified (gain of 10,000), and digitized at 1 kHz through differential current amplifiers. Using custom software written in Matlab (MathWorks, Natick, MA), the continuous EMG signals were manually parsed into segments, each containing a single behavioral episode of jumping, successive swimming, kicking, walking cycles. The parsed EMG data were then high-pass filtered (window-based finite impulse response (FIR); filter with cutoff frequency of 50 Hz and order 50) to remove any movement artifacts. The data were then rectified, low-pass filtered (FIR; filter with

cutoff frequency of 20 Hz and order 50) to remove noise, and integrated over 10 ms intervals.

Data analysis

Analysis step I: separate extraction of synergies

Extracting time-invariant muscle synergies. To extract synchronous, time-invariant muscle synergies that capture the characteristic of each motor behavior, a nonnegative matrix factorization algorithm (NMF, Lee and Seung, 1999; Lee and Seung, 2001) was applied to EMG data set of each motor behavior. The algorithm starts with random nonnegative synergies, vectors whose dimensions are the same as the number of recorded muscles (i.e., 12-13), and coefficients that have the temporal information of the EMG sequence. Then, the algorithm minimizes the total reconstruction error by iterating a coefficient update step and a synergy update step based on multiplicative update rules. A convergence to the optimization was determined if the increase of the reconstruction R^2 was $< 5x10^{-5}$ for five consecutive iterations. To minimize the probability of finding local minima, the optimization was repeated twenty times and the solution with the highest R^2 was selected (d'Avella and Bizzi, 2005).

Measuring the goodness of EMG reconstruction by a linear combination of synergies. The EMG patterns and the residuals of the reconstruction of the patterns by a combination of synergies are multivariate time-series. Thus, a measure of the goodness of the reconstruction, typically a ratio of two variances, must be defined using a multivariate measure of data variability. Here, the "total variation" (Mardia et al., 1979), defined as the trace of the covariance of the muscle activations, was used to define a multivariate R^2 measure as the following:

$$R^2 = 1 - SSE/SST, \quad (1)$$

where SSE is the sum of the squared residuals, and SST is the sum of the squared residual from the mean activation vector, i.e., the total variation multiplied by the total number of samples. Thus, R^2 represents the fraction of total variation accounted for by the synergy reconstruction (d'Avella et al., 2006), and R^2 was used as a measure of goodness for reconstruction of the data.

Selecting a number of synergies. Since there is no exact method to determine the correct number of synergies, a reasonable criterion to choose the number should be consistently applied to each procedure of synergy extraction. Here, the number of synergies whose combination could explain over 90% of total data variance was chosen as the appropriate number for a given data set. This method is valid because the criterion was consistently applied to all data sets for all possible systematic comparisons to address the questions in the present study.

*Measuring synergy similarity***.** Because the time-independent, synchronous synergies extracted by the procedure described above were essentially 12-13 dimensional (i.e., the number of muscles whose activity was recorded) vectors, the cosine of the angle between two normalized synergies could be used as a measure of their similarity. In order to compare two normalized synergies, the scalar product between the two normalized vectors w1 and w2 representing the two synergies was calculated. In addition, the baseline similarity was determined by the 95^{th} percentile of the chance similarity for each pair of random synergies. These random synergies were generated by sampling the empirical distribution of the muscle activation in the dataset from which the real synergies were extracted.

Comparing two synergy sets. With two sets of synergies extracted from two EMG data sets, respectively, all possible matching of the two synergy sets (from different animals or different behaviors) were compared by: (1) computing the similarities between any possible matching pairs of synergies in two different synergy sets, (2) counting the number of pairs with a similarity above the chance level generated by a simulation, (3) selecting the best-matching scalar products (i.e., the maximal sum of scalar products between two sets of synergies) between the two sets of synergies, (4) if multiple synergies from one set was matched to the same synergy in the other set, isolating all multiply-matched and unmatched synergies, (5) calculating the total scalar product of every possible matching combination between these two sets of isolated synergies, and (6) eventually, finding the best match that results in the maximum total scalar product. The number of shared synergies (nss), the number of best-matching scalar products greater than the chance level, was used as a measure of similarity between two different synergy sets. Random synergies were generated by sampling the empirical distribution of the activation amplitudes of each muscle in the dataset from which

the synergies were extracted. Then the similarity between the best-matching pairs among 2,000 sets of random synergies was compared. Eventually, the 95th percentile of the chance similarity for each pair was used as a chance level of similarity between two sets of synergies (Cheung et al., 2005; d'Avella and Bizzi, 2005).

Analysis step II: simultaneous extraction of synergies from pooled data

Extracting time-invariant muscle synergies. In *the stage I analysis*, synergies were extracted separately from the data sets recorded before and after spinalization or transection. However, there are possible shortcomings of the separate extraction method; the synergies extracted from either data set may not actually span a common subspace of EMGs of intact and reduced preparations, and separate extraction of synergies performed in *the stage I* may be expected to underestimate the number of synergies utilized in the execution of natural and brainstem (or medullary) movements, especially if the activation of two synergies tend to co-vary within one of the two data sets (Cheung et al., 2005). Thus, the second step of analysis was performed.

The model of EMG data in this stage of analysis can be represented as follows:

$$\begin{aligned} \boldsymbol{d}^{IN}(t) &= \sum_{i}^{N^{sh}} c_i^{sh\_IN}(t)\, \boldsymbol{w}_i^{sh} + \sum_{i}^{N^{sp\_IN}} c_i^{sp\_IN}(t)\, \boldsymbol{w}_i^{sp\_IN}; \\ \boldsymbol{d}^{RE}(t) &= \sum_{i}^{N^{sh}} c_i^{sh\_RE}(t)\, \boldsymbol{w}_i^{sh} + \sum_{i}^{N^{sp\_RE}} c_i^{sp\_RE}(t)\, \boldsymbol{w}_i^{sp\_RE}; \end{aligned} \qquad (2)$$

where $\boldsymbol{d(t)}$ represents the EMG data at time t, $\boldsymbol{w}_i$ is a 12-13 dimensional vector denoting the i-th synergy, $c_i(t)$ is the time-varying scalar activation coefficient for $\boldsymbol{w}_i$, N is the total number of synergies extracted, the superscripts "*IN*" and "*RE*" stand for data recorded from intact and reduced (i.e., either brainstem or medullary) preparations, respectively, and "*sh*" and "*sp*" stand for synergies shared between the two data sets and synergies specific to either data set, respectively. For example, "*sp_IN*" refers to synergies intact data-specific, while "*sp_RE*" refers to synergies brainstem or medullary data-specific. The coefficients, $c_i^{sh\_IN}(t)$ and $c_i^{sh\_RE}(t)$ contribute to the data recorded from intact and reduced preparations, respectively. In addition, the total number of synergies of behaviors is the sum of the number of shared and

dataset-specific syneriges; for example, the total number of synergies for medullary behaviors is the sum of the number of shared and medullary data-specific synergies (i.e., N for medullary data set = $N^{sh} + N^{sp\_Medullary}$; Cheung et al., 2005).

The modification of the NMF algorithm in this stage of analysis is possible for the characteristic of the NMF multiplicative update rule; by setting the relevant initial synergy coefficients as zero, the specific synergies can explain only one of the two data sets. To remove a bias of the number of data samples in this stage of analysis, equal numbers of EMG data samples recorded from the intact and reduced preparation were pooled together and used for synergy extraction. The synergy and its corresponding matrices used in the analysis are following:

$$D^{all} = [D^{IN} | D^{RE}] = W^{all.} C^{all};$$

$$W^{all} = [W^{sh} | W^{sp\_IN} | W^{sp\_RE}], \; C^{all} = \begin{bmatrix} C^{sh\_IN} & C^{sh\_RE} \\ C^{sp\_IN} & 0 \\ 0 & C^{sp\_RE} \end{bmatrix}, \quad (3)$$

where D, C, W are matrix forms of the corresponding variables, and "*all*" indicates data sets recorded from both intact and reduced preparations.

Estimating the dimensionalities of subspaces shared between sets of intact and brainstem (or medullary) synergies. To choose the appropriate number of shared synergies (N^{sh*}), N^{sh} progressively increased from one to the smaller of the number of either N^{IN} or N^{RE}. As N^{sh} increases one by one, the remaining shared subspace dimensionality of intact data-specific and brainstem (or medullary) data-specific synergies decreases and eventually falls below a threshold. Thus, the correct number of shared synergies (N^{sh*}) can be indicated by the N^{sh} at which there is minimal overlap between the subspaces spanned by the intact data-specific and brainstem (or medullary) data-specific synergies. The degree of this overlap between the specific synergies was quantified as a dimensionality value by finding the number of principal angles with cosines > 0.9. The smallest N^{sh} with a mean shared dimensionality between the specific synergies (averaged across 20 repetitions) below 0.25 was taken to be the correct number of shared synergies. All the procedure of extracting shared and specific synergies originates in

the ideas of data analysis shown in Cheung et al., 2005.

Estimating correct numbers of intact and brainstem (or medullary) synergies. As in the steage I analysis, I chose the total numbers of intact and brainstem synergies (the ***intact vs. brainstem*** condition) or intact and medullary synergies (the ***intact vs. medullary*** condition) that resulted in about 90% reconstruction R^2. This criterion enables a set of synergies of the stage II analysis to explain the intact and brainstem or medullary data sets as much as *the stage I* solution does (Cheung et al., 2005).

RESULTS

In this study, I investigated the anatomical and functional organization of the muscle synergies underlying natural motor behavior. I collected and analyzed EMG data from six frogs. In the ***intact vs. brainstem*** condition, I recorded the EMGs from three intact frogs during jumping (58, 62, and 87, respectively), swimming (328, 374, and 282), kicking (66, 48, and 30), and walking (56, 42; no performance in frog b3). After the transection at the level of the caudal end of the third ventricle, the "brainstem" animals performed jumping (47, 35, and 107), swimming (130, 142, and 242), kicking (90, 48, and 149), and walking (11 and 30; no performance in frog b3). In the ***intact vs. medullary*** condition, EMGs from three intact frogs were recorded during jumping (83, 125, and 98, respectively), swimming (84, 420, and 373), kicking (32, 56, and 104), and walking (61 and 85; no performance in frog m1). After the transection at the level of the caudal end of the pons, I collected EMGs during kicking (90 and 64; no performance in frog m1), and walking (51 and 96; no performance in frog m2).

EMG data recorded before and after transection

Figures 2 and 3 show representative examples of EMGs recorded during jumps, swims, kicks, and walks (Figure 2 for jumps and swims; Figure 3 for kicks and walks) from frog b2 before and after the transection at the level of rostral midbrain. Note that multiple muscles are coactivated as a group during certain phases in a behavioral episode. For instance, as shown in Figure 2*A*, an EMG segment during a natural jump in an intact animal is divided into three phases, marked as *a*, *b*, and *c* distinguished by two vertical lines. The division of EMGs into phases is for ease of visual inspection. During phase *a*, all 13 muscles are

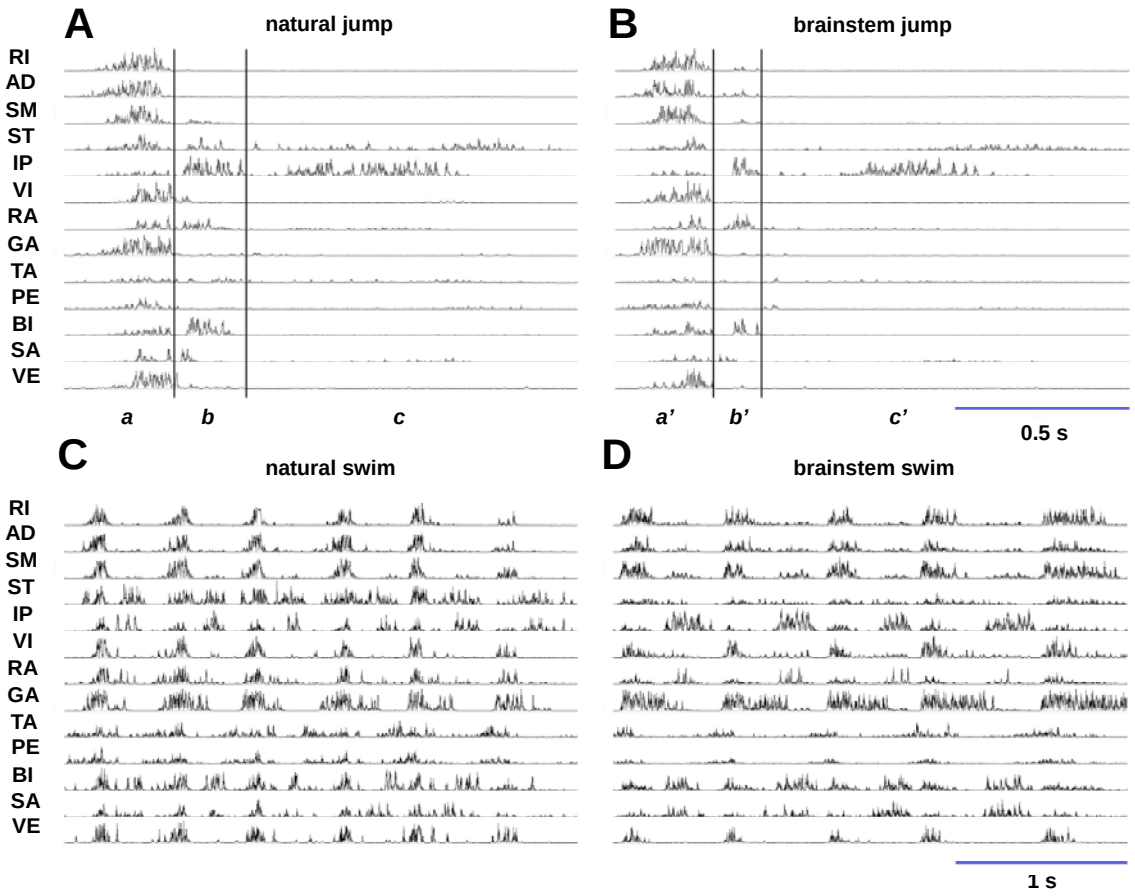

Figure 2. Examples of EMG data recorded during jumps and swims in experiments of the ***intact vs. brainstem*** condition in frog b2. The names of 13 muscles are shown on the left side of Figs. 2*A* and 2*C* in an abbreviated form. The EMGs are high-pass filtered (window-based finite impulse response (FIR); filter with cutoff frequency of 50 Hz and order 50) to remove movement artifacts, and then rectified. EMGs of a jump episode ***A***, before transection and ***B***, after transection at the level of the caudal end of the third ventricle. The behavioral episodes of jumps both before and after the transection (Figs. 2*A* and 2*B*) have a similarity in the sense that the EMGs recorded during the behavior have three different characteristic phases (*a*, *b*, and *c* in natural jumps; *a'*, *b'*, and *c'* in brainstem jumps; phases distinguished by two vertical lines in each subplot) with a variation of amplitude and duration of muscle activation. The division of EMGs into phases is for ease of visual inspection. Phases *a*, *b*, and *c* correspond to phases *a'*, *b'*, and *c'*, respectively. EMGs of a sequence of swim ***C***, before transection and ***D***, after transection at the same level in the identical animal (frog b2).

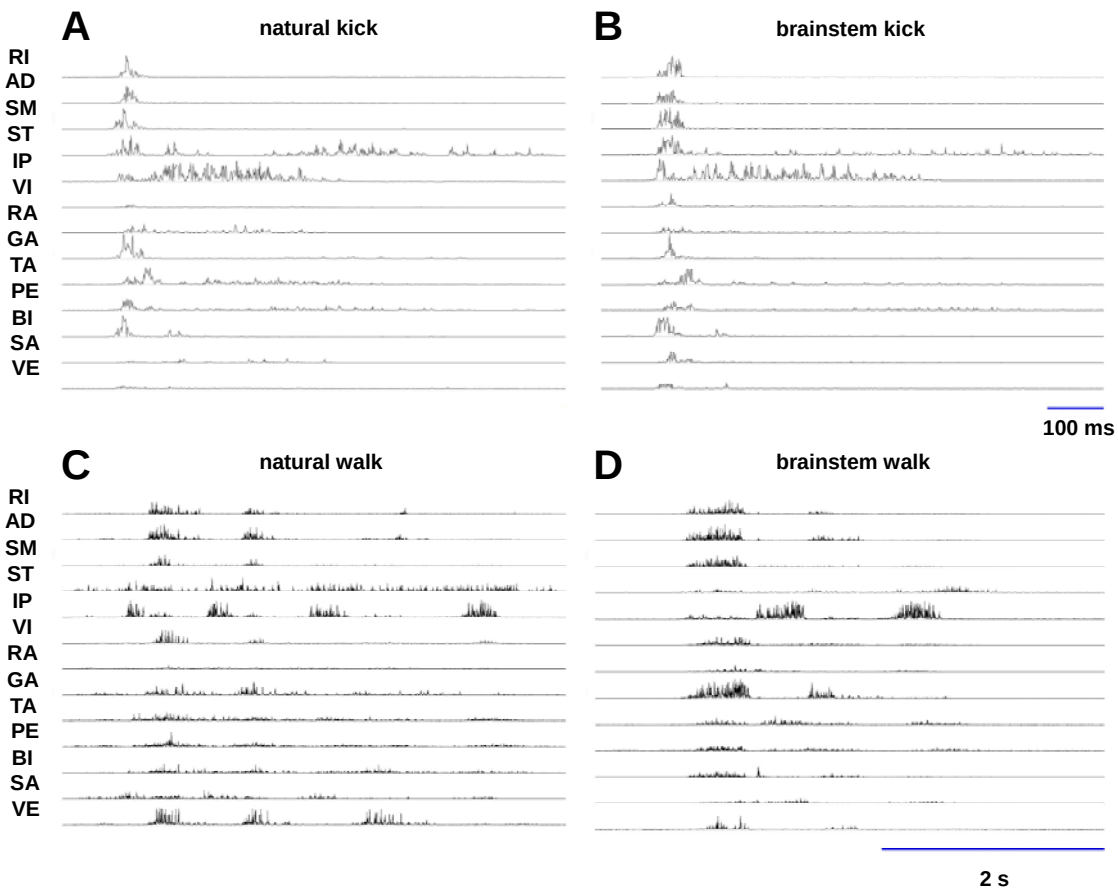

Figure 3. Examples of EMG data recorded during kicks and walks in experiments of the ***intact vs. brainstem*** condition in frog b2. The names of 13 muscles are shown on the left side of Figs. 3*A* and 3*C* in an abbreviated form. The EMGs are high-pass filtered (window-based finite impulse response (FIR); filter with cutoff frequency of 50 Hz and order 50) to remove movement artifacts, and then rectified. EMGs of a kick episode ***A***, before transection and ***B***, after transection at the level of the caudal end of the third ventricle. EMGs of a sequence of steps (walk) ***C***, before transection and ***D***, after transection at the same level in the identical animal (frog b2).

activated, while only ST, IP, VI, RA, BI, and SA are activated in phase *b*. Phase *c* is characterized by the activities of ST and IP. The EMG episode evoked after the transection has three subdivisions, labeled as *a'*, *b'*, and *c'*, each corresponding to each phase (*a*, *b*, or *c*) of a jump episode before the transection, as demonstrated in Figure 2*B*. The EMGs recorded from the brainstem preparation appear to be characterized by activation of the same muscle groups involved in the EMGs of the intact preparation. For instance, during phase *b'*, which is analogous to phase *b*, ST, IP, VI, RA, BI, and SA are activated, whereas mainly ST and IP show activation during phases *c* and *c'*. However, while the muscle members activated during a certain phase of the EMG episode are identical before and after transection, the duration and amplitude of the activation are different. Thus, some features of muscle activation during jumps tend to be kept invariant after the transection with a variation of the duration and amplitude of the activation.

Similarly, visual inspection of a course of muscle activation suggests that synergistically activated muscle groups during swimming remain invariant after the transection to disconnect the brainstem from the supra-brainstem networks. Figure 2*C* shows successive cycles of swimming observed in intact frog b2. The muscles RI, AD, SM, VI, and VE are coactivated as a group in the behavioral episode of swims. TA and PE are activated synergistically, while ST or IP tends to be distinguished from other muscles due to the different phases and the duration of their activations. Most interestingly, these coactivation patterns of muscles as a group in an intact frog b2 are also observed in the episode after the transection in a brainstem frog b2 as shown in Figure 2*D*.

The tendency that some features of synergistically activated muscle groups are kept consistent is also found in other motor behaviors including kicking and walking (Figure 3). Furthermore, even after the transection at a more lower level (i.e., at caudal end of the pons, as shown in Figure 4), I observed the coactivation of muscles as a group with invariant activation features, even though there is a modification of durations and amplitudes of muscle activation. For instance, the EMGs recorded during kicking and walking in a medullary preparation (frog m3) (Figs. 4*B* and 4*D*) are characterized by longer durations and larger amplitudes of muscle activation, in general, than those of the EMG activities observed before the transection in the intact preparation (Figs. 4*A* and 4*C*). These overall findings motivated me to investigate similarities and differences between muscle synergies in intact and reduced preparations (brainstem or medullary preparations) to assess the extent of

modulation of muscle synergies from supra-brainstem or supra-medullary centers. If muscle synergies extracted from EMG patterns obtained from reduced preparations show important similarities with the muscle synergies underlying motor pattern recorded from the corresponding muscles during motor behaviors in intact animals, this observation may support the idea that key elements of muscle synergies are programmed by neural circuitries at a level caudal to the transection.

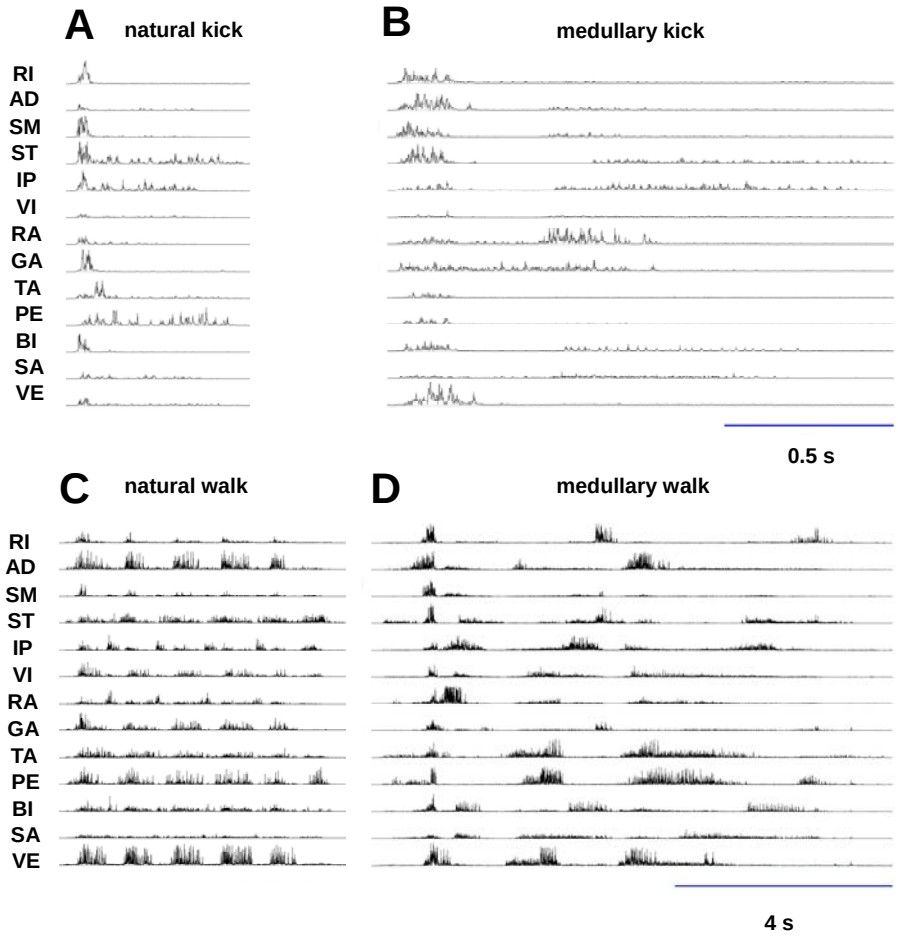

Figure 4. Examples of EMG data recorded during kicks and walks in experiments of the ***intact vs. medullary*** condition in frog m3. The names of 13 muscles are shown on the left side of Figs. 4*A* and 4*C* in an abbreviated form. The EMGs are high-pass filtered (window-based finite impulse response (FIR); filter with cutoff frequency of 50 Hz and order 50) to remove movement artifacts, and then rectified. EMGs of a kick episode ***A***, before transection and ***B***, after transection at the level of the caudal end of the pons. EMGs of a sequence of steps (walk) ***C***, before transection and ***D***, after transection at the same level in the identical animal (frog m3).

Low dimensionality of individual natural, brainstem, and medullary behaviors

To assess the complexity of motor behaviors before and after transection at a certain level, sets of time-invariant muscle synergies used in the execution of each behavior in each frog were extracted by the NMF algorithm (see Materials and Methods). The number of extracted synergies in each data set ranged from one to eight. I used the R^2 values, the fraction of the total variation in the data explained by a combination of the synergies in each EMG data set, as a measure of the goodness of reconstruction of the corresponding EMGs.

Figure 5 shows plots of R^2s as a function of synergies for individual data sets recorded from intact frogs, along with the data recorded after transection in "brainstem" preparations. As the number of synergies increased, R^2 increased, ranging from an average of 0.4837 with one synergy to an average of 0.9767 with eight synergies. Note that in all the individual data sets recorded before and after the transection, about 90% of data variance in the original EMGs was explained by a combination of three to six synergies. A significantly smaller number of synergies than the dimensionalities of the muscles (12 or 13) explained a large fraction of the total data variance of EMGs, suggesting that data from both the intact animals and "brainstem" preparations possess low and comparably similar dimensionalities.

To verify the significance of the extracted synergies, the R^2 levels for the synergies extracted from the original data (red curves in Figure 5) were compared to the R^2 values for the synergies extracted from reshuffled, structureless data (blue curves in Figure 5). As seen in Figure 5, this comparison indicated that, for all individual behavioral cases (jumping, swimming, kicking, and walking from intact or reduced preparations), the R^2 values for three to six synergies extracted from the original data were significantly higher than the R^2 values for the same number of synergies extracted from the reshuffled data. Therefore, the synergy extraction algorithm used here successfully captured the amplitude relationship among activation of major muscles in the frog hindlimb. Since the amplitude distributions for individual muscles were the same in the original and reshuffled data, the synergy structure indicates not simply the amplitude distribution for each individual muscle but the spatial structure of muscle activity (d'Avella and Bizzi, 2005).

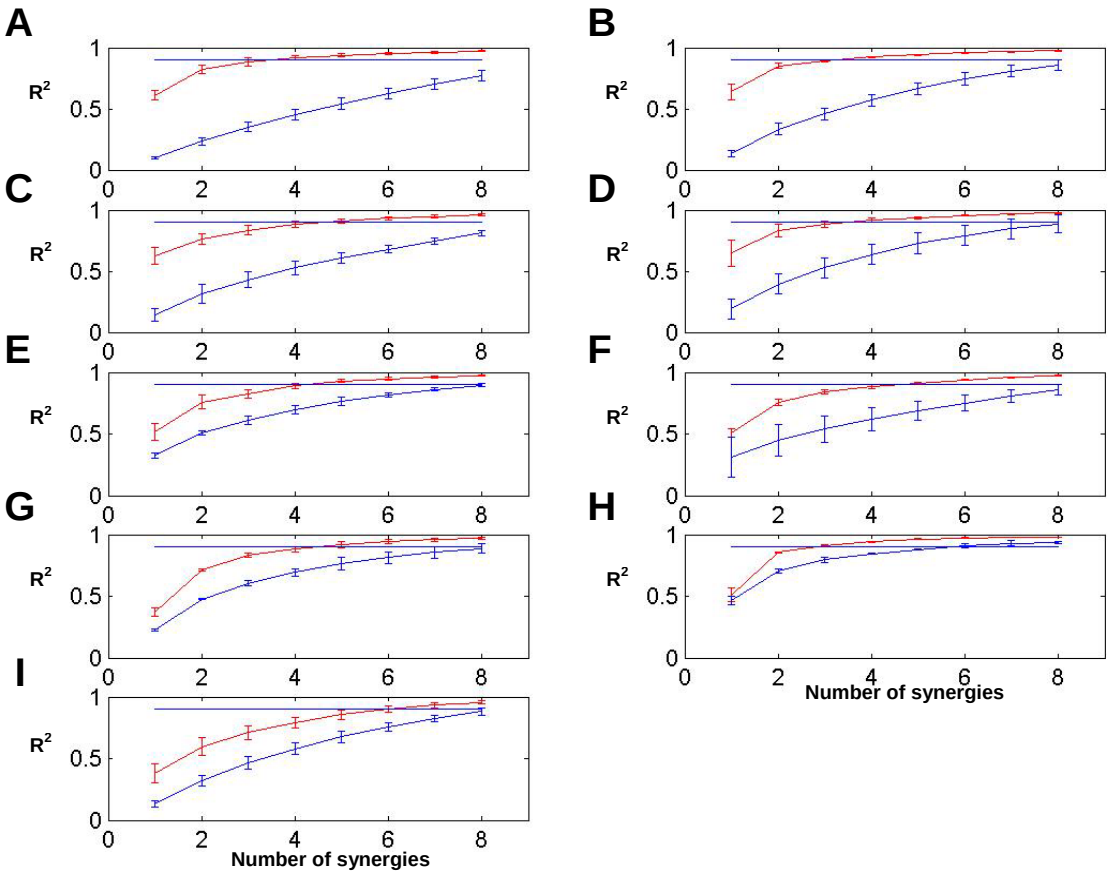

Figure 5. The fraction of total EMG data variation displayed as a function of the number of extracted synergies. In each subplot, the curves show that the percentage of data variance accounted for by the synergy combination (R^2; mean±STD; n=20) increases as the number of synergies extracted increases. The red curves indicate how real synergies extracted from the original EMG data set reconstruct the original data, while the blue curves illustrate how synergies extracted from the reshuffled EMGs reconstruct the structureless data. Note that the reconstruction R^2s for original EMG signals are significantly higher than the R^2s for reshuffled EMGs, suggesting that the structure of extracted synergies is not a result of a bias of the extraction algorithm used in the analysis. Reconstruction R^2 curves ***A***, for jumps in three intact frogs, ***B***, for jumps after transection in three brainstem frogs, ***C***, for swims in three intact frogs, ***D***, for swims after transection in three brainstem frogs, ***E***, for kicks in three intact frogs, ***F***, for kicks after transection in three brainstem frogs, ***G***, for walks in two intact frogs, ***H***, for walks after transection in two brainstem frogs, and ***I***, for medullary motor behaviors in three medullary frogs.

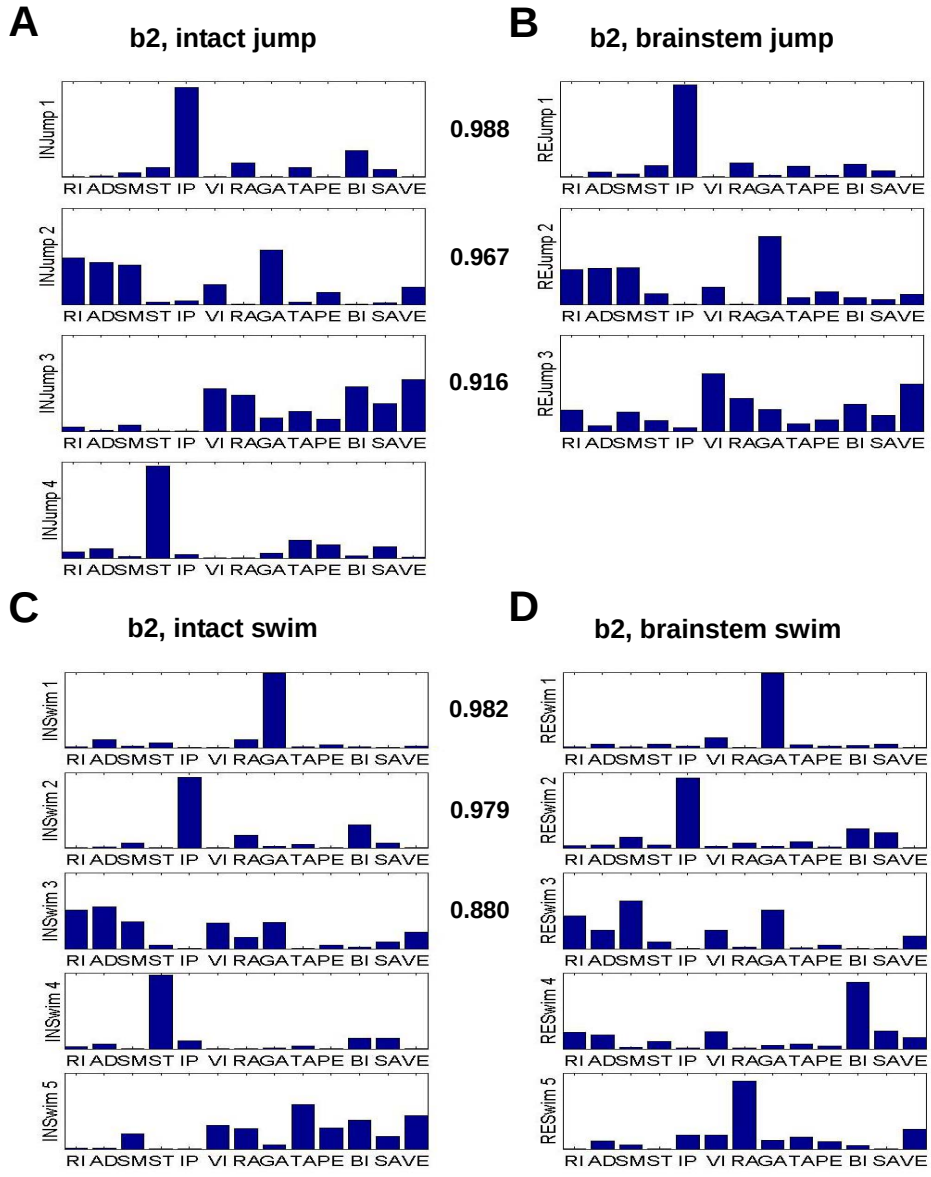

Figure 6. Examples of synergies extracted separately from each behavioral EMG data set recorded during jumping and swimming before and after transection at the level of the caudal end of the third ventricle of frog b2. The first three of four (Fig. 6*A*) or the first three of five (Fig. 6*C*) synergies for natural movements are matched to the corresponding number of the synergies in the "brainstem" preparation (Figs. 6*B* and 6*D*), which result in the maximal summation of scalar products between two synergy sets. The numbers between the two synergies in Figure 6 are the statistically significant scalar products (p<0.05), demonstrating how similar two synergies are. The comparisons of synergies in jumps (Figs. 6*A* and 6*B*) and in swims (Figs. 6*C* and 6*D*) show that three out of four synergies for jumps and three out of five synergies for swims in an intact preparation are well preserved after transection at the level of the third ventricle.

Experiment I. Muscle synergies underlying intact and brainstem movements

Observation of the structure of muscle synergies in movements before and after the transection

Figures 6 and 7 show an example of four pairs of intact and brainstem synergy sets in frog b2. Each synergy underlying natural movements in the intact animal was reordered for plotting to be matched to the synergy observed in the brainstem preparation. The set of matched synergies made the best-matching (i.e., maximal summation) scalar product. Figs. 6*A* and 6*B* demonstrate that a set of four synergies underlying jumps in the intact animal and a set of three synergies for "brainstem" jumps (i.e., jumps observed in brainstem preparations). In Fig. 6*A*, in the intact animal, the first three synergies in jumps are also present in the brainstem preparation during the same behavior.: (1) a hip flexor-dominant synergy, (2) hip extensors, knee flexors, and ankle extensor-dominant synergy, and (3) a hip flexor and a knee extensor-dominant synergy, respectively. The fourth synergy underlying jumps in the intact preparation is dominated by ST, a hip extensor and a knee flexor, which is not shown as a synergy for "brainstem" jumps. Note that not all, but a majority of synergies utilized in the execution of natural movements in intact preparations underlie the corresponding motor behaviors observed in brainstem preparations.

The first three synergies underlying kicks in Fig. 7*A* have similarity in the structure with the first three "brainstem" kick synergies: (1) IP, a hip flexor-dominant synergy, (2) ST, a hip extensor and a knee flexor-dominant synergy, and (3) hip extensors, knee flexors, and an ankle extensor-dominant synergy, respectively. Similarly, in Fig. 7*C*, the first three walk synergies in an intact preparation appear as synergies in "brainstem" walks: (1) IP, a hip flexor-dominant synergy, (2) GA, a knee flexor and an ankle extensor-dominant synergy, and (3) ST, a hip extensor and a knee flexor-dominant synergy, respectively. In summary, a significant portion of muscle synergies before and after the transection are almost identical with some variability in the amplitude and duration of muscle activations in each synergy.

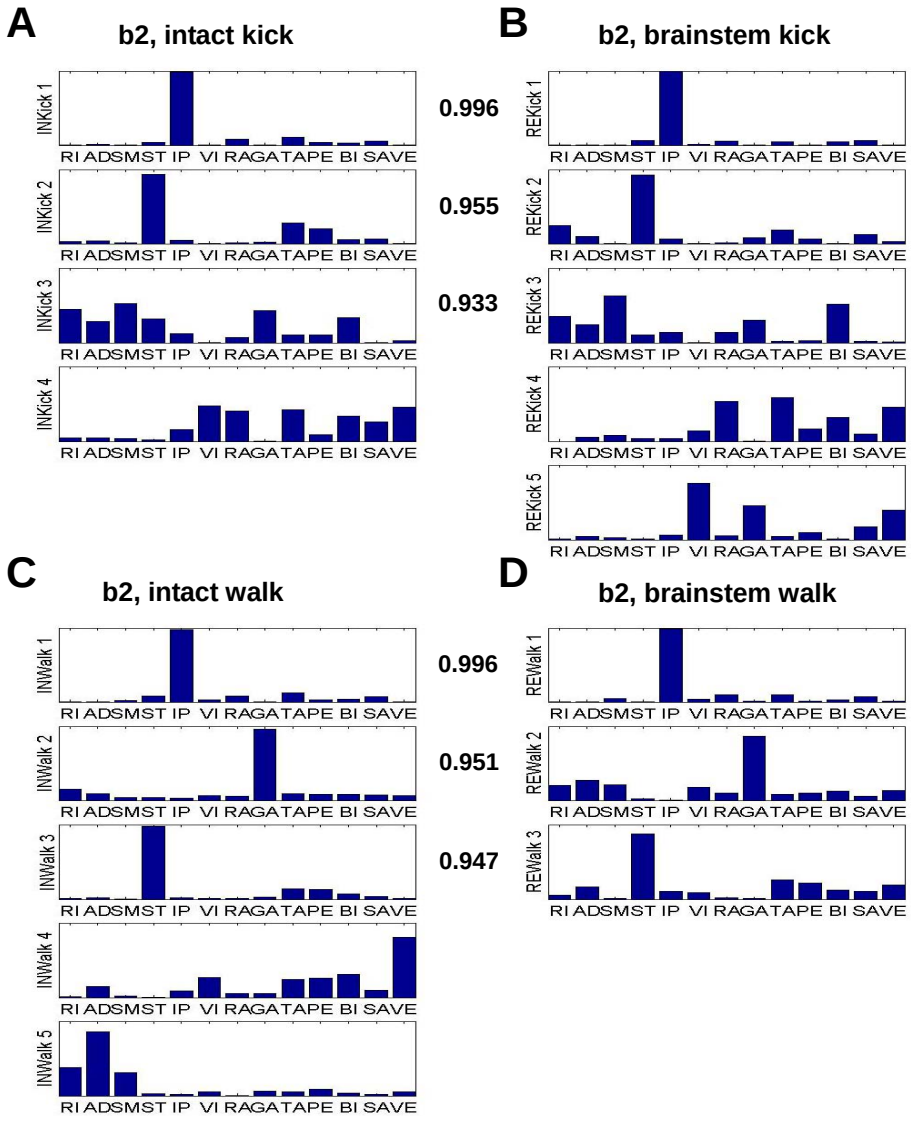

Figure 7. Examples of synergies extracted separately from each EMG data set recorded during kicking and walking before and after transection at the level of the caudal end of the third ventricle of frog b2. The first three of four (Fig. 7*A*) or the first three of five (Fig. 7*C*) synergies for natural movement are matched to the corresponding number of the synergies for brainstem movements (Figs. 7*B* and 7*D*), which make the best-matching scalar product. The numbers between the two synergies in Figure 7 are the statistically significant scalar products (p<0.05), demonstrating how similar two synergies are. The comparisons of synergies in kicks (Figs. 7*A* and 7*B*) and in walks (Figs. 7*C* and 7*D*) show that three out of four synergies for natural kicking and three out of five synergies for natural walking are well preserved after transection at the level of the third ventricle, respectively.

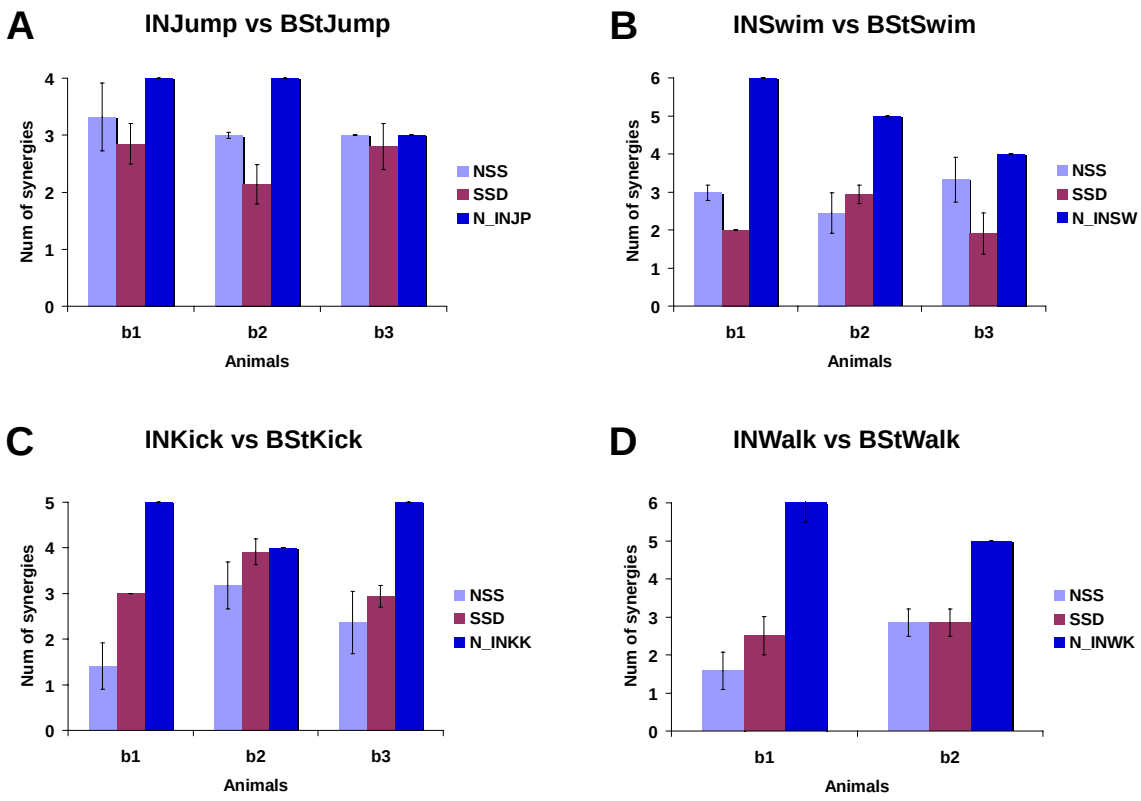

Figure 8. A significant portion of synergies for individual natural movements, with interanimal variability, is well preserved after transection at the level of the caudal end of the third ventricle (IN is an indication of behavior recorded from an intact preparation; BSt, "brainstem" behavior; NSS, number of shared synergies; SSD, shared subspace dimensionalities; N_INJP, number of synergies for jumping in an intact preparation; N_INSW, number of synergies for swimming in an intact preparation; N_INKK, number of synergies for kicking in an intact preparation; N_INWK, number of synergies for walking in an intact preparation). NSS and SSD are two quantitative parameters indicating how many synergies are common in natural and "brainstem" movements. For example, in Fig. 8*A*, in the case of frog b1, about three out of four synergies for jumping in the intact state (mean±STD, n=20) are similar to synergies for jumping in the state of brainstem preparation (NSS), and about three out of four subspace dimensionalities for dataset recorded during jumping in the intact state (mean±STD, n=20) are similar to dimensionalities of subspace spanned by data recorded during jumping in the state of brainstem preparation (SSD). Comparisons of synergies for jumping (Fig. 8*A*), for swimming (Fig. 8*B*), for kicking (Fig. 8*C*), and for walking (Fig. 8*D*) before and after the transenction. Note that there is interanimal variability in terms of NSS and SSD across all four (***A***, ***B***, ***C***, and ***D***) comparisons.

Analysis in step I: estimating similarity of muscle synergies

To calculate how similar synergies are before and after the transection at the rostral brainstem, two quantitative measures were computed: (1) the number of shared synergies (NSS) and (2) the shared subspace dimensionality (SSD) (Cheung et al., 2005). I used two measures of similarity to reconfirm the similarity between the intact and "brainstem" EMG data sets.

Since a synergy was defined as a vector, scalar products between a pair of intact and "brainstem" synergy sets from an identical animal specify how similar two synergies are. As shown in Figures 6 and 7, the results of scalar products that were statistically significant ($p<0.05$) are shown between the two sets of synergies: in intact frog b2, three synergies in jumps, three synergies in swims, three synergies in kicks, and three synergies in walks are shared with the corresponding numbers of "brainstem" synergies for corresponding behaviors. Here, I refer to the number of best-matching scalar products as the NSS. A summary of the numbers is in Table 1.

Furthermore, the degree of overlap between the subspaces spanned by the sets of synergies utilized in the execution of natural motor behaviors and synergies observed in "brainstem" preparation (SSD) was calculated by computing principal angles (Golub and van Loan, 1983). Figure 8 shows the SSD between the two sets of the synergies found in intact and brainstem preparations (Fig. *8A*, synergies for jumps; Fig. *8B*, synergies for swims; Fig. *8C*, synergies for kicks; and Fig. *8D*, synergies for walks) across all animals in which EMG data were recorded. On average, three out of four, two out of four, and three out of three dimensions of the subspaces spanned by the synergies in the execution of jumps in intact frogs b1, b2, and b3, respectively, are shared with their corresponding subspaces spanned by synergies utilized in the execution of jumps in brainstem frogs b1, b2, and b3. Three out of six, three out of five, and two out of four dimensions of the subspaces spanned by a set of synergies in swims observed in the three intact animals are shared with the subspaces spanned by synergies for swims in the three "brainstem" animals. For kicking, three out of five, four out of four, and three out of five dimensions of subspaces spanned by synergies in the three intact animals are shared with the subspaces spanned by synergies observed after the transection in brainstem animals. In walks, three out of six and three out of five dimensions of subspaces spanned by synergies observed in two intact animals (frog b1 and

Table 1. Summary of *stage I analysis*: estimating the number of synergies shared between the synergy sets utilized in the execution of movements in intact and "brainstem" preparations

Frog	Comparison Condition	N_IN	N_BSt	NSS	SSD	Similarity	Subangle	R^2 (%)	
								Intact	Brainstem
b1	INJump vs BStJump	4.000±0.000	4.050±0.218	3.318±0.594	2.850±0.358	0.895±0.097	0.215±0.103	0.908±0.000	0.918±0.008
b2	INJump vs BStJump	4.000±0.000	3.000±0.000	2.998±0.050	2.140±0.347	0.952±0.037	0.164±0.075	0.905±0.000	0.903±0.000
b3	INJump vs BStJump	3.000±0.000	4.000±0.000	3.000±0.000	2.800±0.401	0.890±0.164	0.164±0.123	0.920±0.001	0.924±0.007
b1	INSwim vs BStSwim	6.000±0.000	3.050±0.218	2.980±0.199	2.000±0.000	0.748±0.178	0.178±0.116	0.919±0.000	0.906±0.005
b2	INSwim vs BStSwim	5.000±0.000	5.000±0.000	2.445±0.527	2.935±0.247	0.948±0.045	0.216±0.111	0.904±0.001	0.919±0.002
b3	INSwim vs BStSwim	4.000±0.000	4.000±0.000	3.338±0.587	1.903±0.537	0.856±0.100	0.265±0.134	0.911±0.000	0.916±0.005
b1	INKick vs BStKick	5.000±0.000	5.000±0.000	1.408±0.512	3.000±0.000	0.977±0.024	0.230±0.158	0.921±0.000	0.919±0.002
b2	INKick vs BStKick	4.000±0.000	5.000±0.000	3.180±0.513	3.913±0.283	0.964±0.027	0.172±0.132	0.904±0.001	0.914±0.001
b3	INKick vs BStKick	5.000±0.000	5.000±0.000	2.463±0.689	2.940±0.238	0.921±0.036	0.172±0.106	0.921±0.001	0.904±0.000
b1	INWalk vs BStWalk	5.500±0.500	3.000±0.000	1.583±0.494	2.500±0.501	0.962±0.045	0.181±0.158	0.915±0.014	0.920±0.000
b2	INWalk vs BStWalk	5.000±0.000	3.000±0.000	2.850±0.358	2.850±0.358	0.957±0.036	0.087±0.064	0.932±0.005	0.908±0.000

Two parameters (NSS, number of shared synergies; SSD, shared subspace dimensionality) are used to estimate the number of common synergies in the exection of natural and "brainstem" movements (N_{IN}, number of synergies for natural movement in an intact preparation, N_{BSt}, number of synergies for movements in a brainstem preparation; all values are mean±STD; n=20)

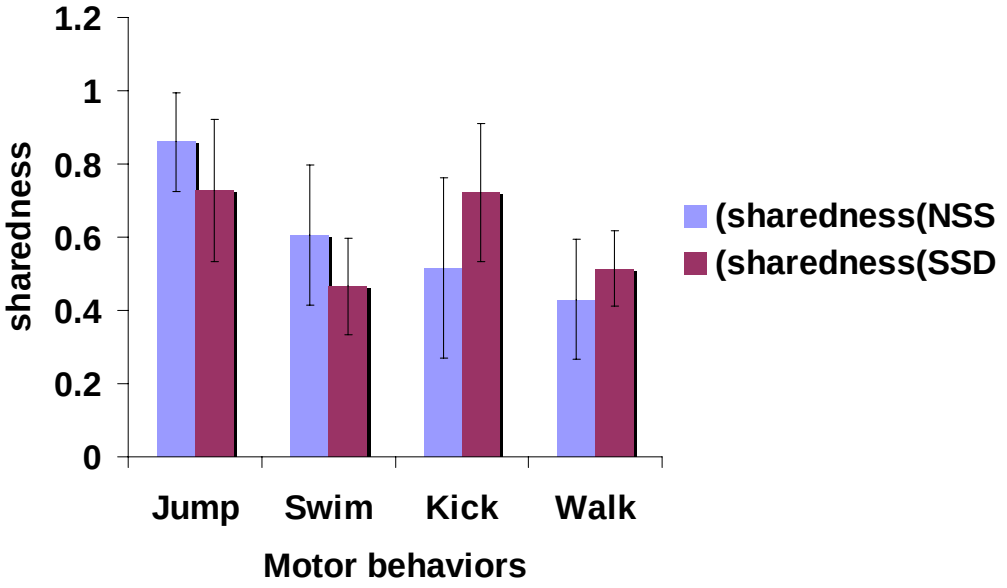

Figure 9. Ratios of the number of shared synergies to the total number of synergies in individual natural motor behaviors across four different comparison conditions (NSS, number of shared synergies; SSD, shared subspace dimensionality). Sharedness represented in the y-axis indicates the ratio of NSS or SSD to the number of synergies for each natural motor behavior observed in all animals recorded (sharedness(NSS) and sharedness(SSD), respectively). All light blue bars indicate the ratio of NSS to the number of synergies in intact animals, while all purple bars mean the ratio of SSD to the number of synergies in intact preparations. Across all four comparisons of natural and brainstem motor behaviors, about over 60% of synergies in intact animals remain invariant after transection and appear as "brainstem" synergies, suggesting that a large portion of synergies in the execution of natural motor behaviors in intact animals is structured by the neural circuits within the brainstem and spinal cord.

b2; no walks performed by frog b3) intersect with subspaces spanned by synergies in brainstem animals. Note that, even though the subspaces spanned by synergies in intact and brainstem preparations are not identical (i.e., completely overlapping with each other), NMF successfully found synergies for four major types of frog motor behaviors (jumping, swimming, kicking, and walking), which span shared subspaces before and after transection. The summary of the *stage I analysis* is shown in Table 1.

Figure 9 shows that sharedness, the ratio of the number of common synergies to the total number of synergies for the four individual intact behaviors, is over 60%, with a variability across different motor behaviors, suggesting that the brainstem and the spinal cord are responsible for structuring a repertoire of muscle synergies utilized in the generation of four major types of natural motor behaviors.

In *stage I analysis*, synergies were extracted from the data sets recorded from intact and brainstem preparations separately, and there are possible shortcomings in the method of separate extraction of synergies (see Materials and Methods). Thus, I performed a second step of analysis.

Analysis in step II: extracting shared and EMG data set-specific synergies

To avoid the limitations of extracting synergies separately from data recorded in intact and "brainstem" preparations, a modified version of NMF (see Materials and Methods) was utilized. In this *stage II analysis*, I concatenated two data sets to be compared and the NMF extracted two types of synergies from the pooled data: one type of synergy was common in both data sets, and the other type was specific to either data set. The characteristic of the NMF multiplicative update rule made it possible to simultaneously extract both shared and data-set specific synergies (i.e., if the initial condition of any synergy coefficient is set as zero, the estimate of the corresponding synergy coefficient is zero after whatever number of iteration in the procedure of synergy extraction).

Figure 10 demonstrates examples of how to estimate the correct numbers of synergies for movements observed in intact and "brainstem" preparations and the number of synergies common in movements of both intact and brainstem preparations. Before running the modified version of the NMF algorithm, the numbers of synergies underlying movements in intact and brainstem preparations and the number of brainstem preparation-specific synergies should be given as inputs in the algorithm. In the *stage II analysis*, the

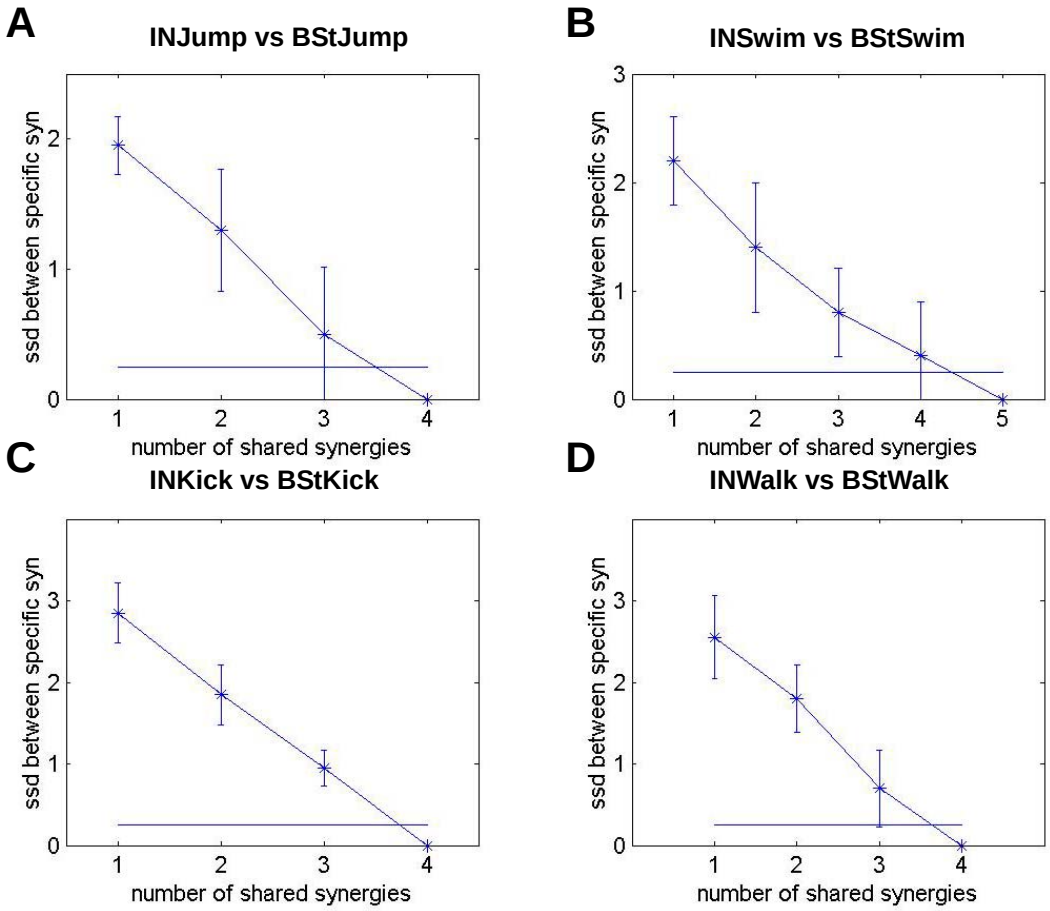

Figure 10. Estimating the number of shared synergies in the *analysis stage II*. As the number of shared synergies (N^{sh}) increases progressively, the dimensionality of the subspace shared between the specific synergies (ssd) underlying EMGs recorded in intact and brainstem preparations decreases. Estimating the correct number of shared synergies in intact and brainstem preparations was done by finding the number of shared synergies at which the specific synergies no longer share a common subspace; that is, at the maximum N^{sh}, the shared dimensionality was defined to be zero. Here the correct N^{sh} was selected as the smallest N^{sh} with a shared dimensionality falling below 0.25. Four out of four synergies for jumps (Fig. 10*A*), four out of five synergies for swims (Fig. 10*B*), four out of four synergies for kicks (Fig. 10*C*), and four out of four synergies for walks (Fig. 10*D*) are similar to synergies underlying EMGs recorded in brainstem preparations.

appropriate numbers of synergies in the execution of movements in intact and "brainstem" preparations were specified in the NMF algorithm as the numbers of synergies that could explain about 90% of the variance of the original EMG data as the set of synergies in the *stage I analysis* could do. As the number of shared synergies progressively increases, it is expected that the dimension of the subspace shared between the "intact" data-specific and "brainstem" data-specific synergies decreases.

In *stage II analysis*, the appropriate numbers of shared synergies were determined when the shared dimensionality became less than a threshold of 0.25 as the number of shared synergies increased. For instance, in Figs. 10*A*-10*D*, when four out of four, four out of five, four out of four, and four out of four shared synergies were extracted, respectively, the remaining shared dimensionality between individual "intact" EMG data-specific and "brainstem" EMG data-specific synergies decreased below 0.25, a threshold. This indicates that there are four out of four, four out of five, four out of four, and four out of four synergies underlying both data sets recorded during from the individual natural and "brainstem" behaviors (jumping, swimming, kicking, or walking).

The same methods described above were applied to data collected from all frogs, and Figure 11 illustrates representative examples of synergies for jumps, swims, kicks, and walks in *stage II analyses*. Interestingly, the synergies extracted at the *stage II analysis* are all matched to those at the *stage I analysis*. For instance, in Fig. 11*A*, sh1 to sh4 synergies for jumps (i.e., synergies underlying jumps performed by both intact and brainstem preparations) are similar to INJump3, INJump4, INJump1, and INJump2, respectively, in Fig. 6*A*; in Fig. 11*B*, sh1 to sh5 synergies for swims are similar to INSwim4, INSwim3+ INSwim5, INSwim2, INSwim1, and BStSwim5, respectively, in Fig. 6*C*. Similarly, in Fig. 11*C*, sh1 to sh4 synergies for kicks are close to INKick2, INKick4, INKick3, and INKick1, respectively, in Fig. 7*A*; in Fig. 11*D*, sh1 to sh4 and sp1 synergies for walks are close to INWalk2, INWalk1, INWalk3, INWalk5, and INWalk4, respectively, in Fig. 7*C*. The summary of the *stage II analyses* across all three animals is shown in Table 2.

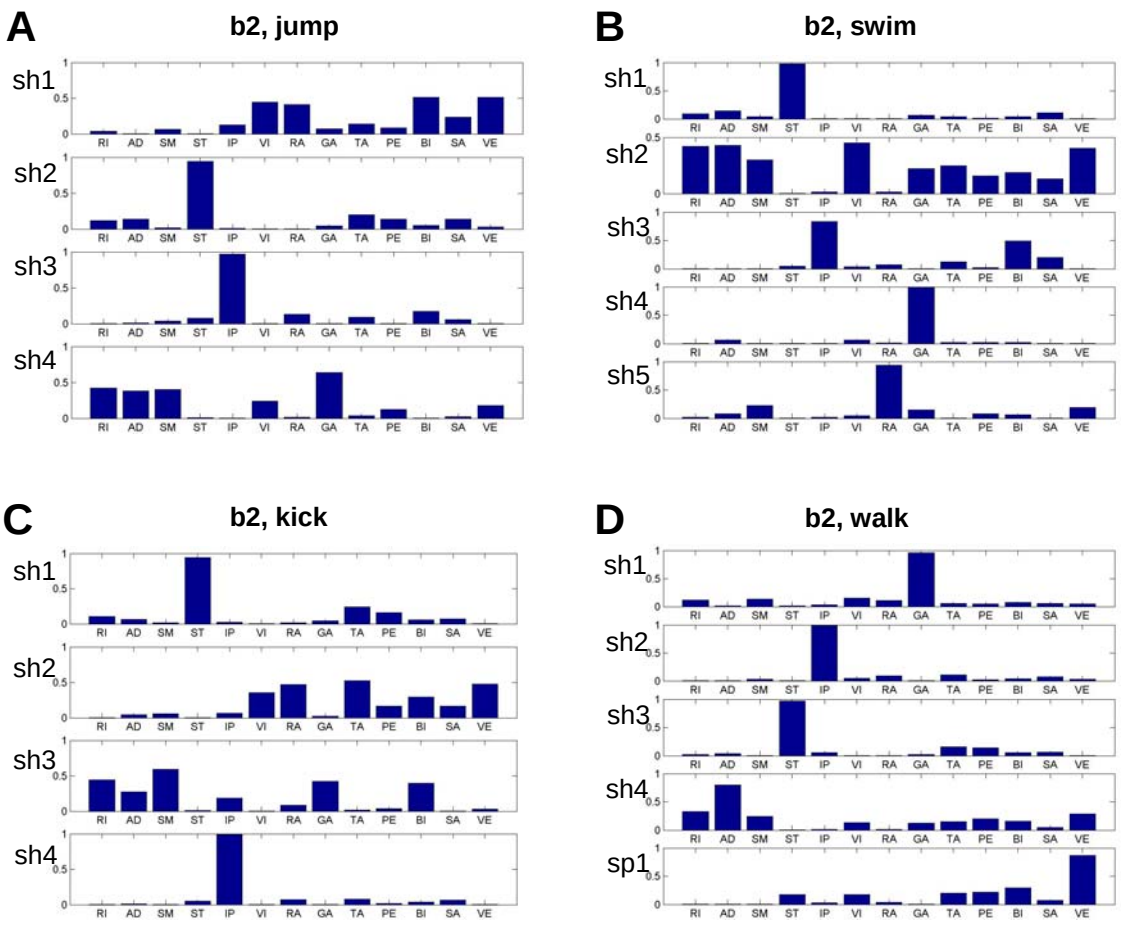

Figure 11. Sets of synergies extracted from the EMGs during four individual natural motor behaviors of frog b2 in the *analysis stage II*. Each synergy represents the balance of activation of muscles recorded. "sh" refers to synergies "shared" by EMGs recorded in intact and brainstem preparations, while "sp" indicates individual "intact" EMG data or "brainstem" EMG data-"specific" synergies. The full terms of the abbreviated muscle names are shown in Materials and Methods. ***A***, A set of four shared synergies for jumps. ***B***, A set of five shared synergies for swims. ***C***, A set of four shared synergies for kicks. ***D***, A set of four shared (first four) and one "intact" EMG data-specific synergies for walks.

Table 2. Summary of *stage II analysis*: estimating the number of synergies shared between sets of synergies for natural and "brainstem" motor behaviors

Frog	Comparison Condition	N_{IN}	N_{BSt}	N_{sh}	N_{sp_IN}	N_{sp_BSt}	R^2 (%)	
							Intact	Brainstem
b1	INJump vs BStJump	5	4	4	1	0	0.911±0.003	0.907±0.005
b2	INJump vs BStJump	4	4	4	0	0	0.898±0.001	0.913±0.001
b3	INJump vs BStJump	3	4	3	0	1	0.919±0.001	0.903±0.003
b1	INSwim vs BStSwim	6	3	3	3	0	0.867±0.006	0.923±0.007
b2	INSwim vs BStSwim	5	6	5	0	1	0.892±0.003	0.908±0.005
b3	INSwim vs BStSwim	5	3	3	2	0	0.891±0.002	0.893±0.000
b1	INKick vs BStKick	5	6	4	1	2	0.917±0.002	0.913±0.010
b2	INKick vs BStKick	4	5	4	0	1	0.899±0.002	0.903±0.002
b3	INKick vs BStKick	5	6	4	1	2	0.904±0.005	0.928±0.006
b1	INWalk vs BStWalk	6	3	3	3	0	0.876±0.010	0.941±0.006
b2	INWalk vs BStWalk	5	4	4	1	0	0.891±0.008	0.949±0.003

See Materials and Methods for details on how to extract synergies in *stage II analysis* (N_{IN}, number of synergies for natural movements in an intact preparation; N_{BSt}, number of synergies for movements observed in a "brainstem" preparation; N_{sh}, number of shared synergies; N_{sp_IN}, number of "intact" EMG data-specific synergies; N_{sp_BSt}, number of "brainstem" EMG data-specific synergies; R^2, percentage of data variance explained by the listed numbers of synergies; all values are mean±STD; no STD indication means zero STD; n=20).

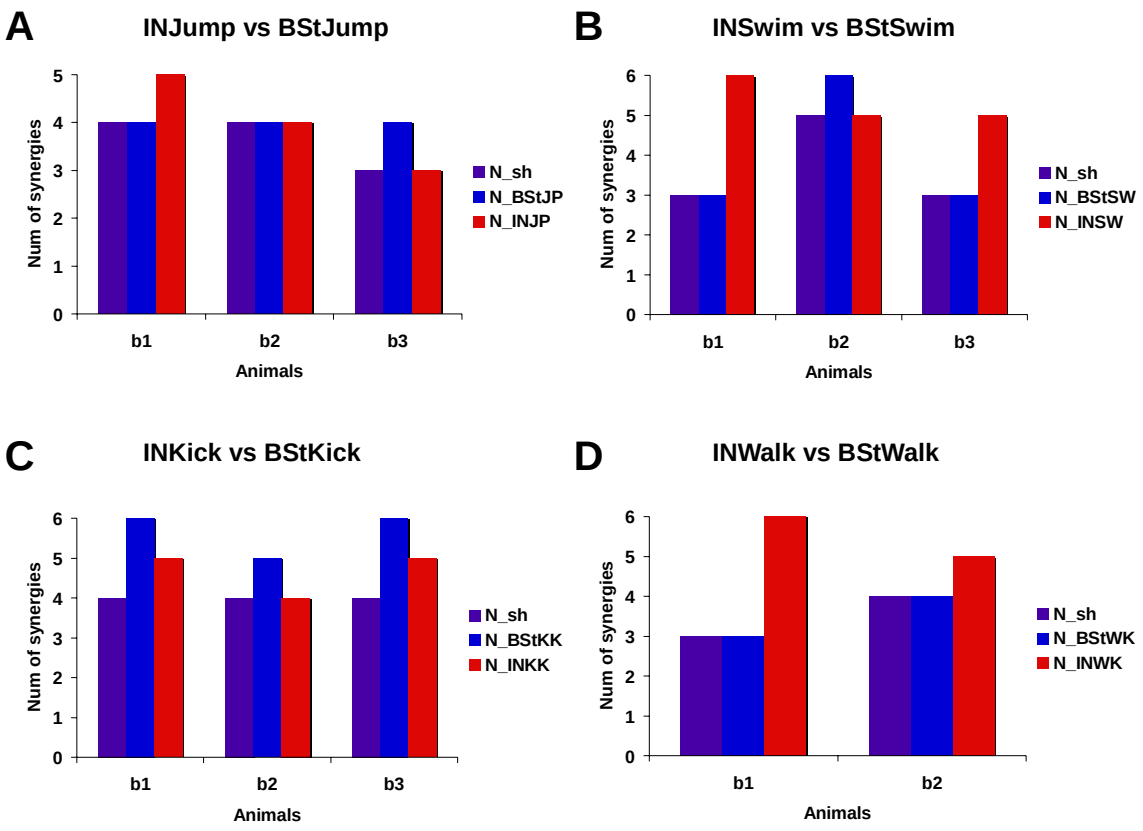

Figure 12. The number of shared synergies (N_sh) and the number of extracted synergies for individual motor behaviors in the *analysis stage II*. Each subplot (***A***, ***B***, ***C***, or ***D***) demonstrates that almost all synergies extracted from an individual intact EMG data set are well preserved after transection at the level of the caudal end of the third ventricle (IN indicates behaviors in intact preparations (e.g., INJump referring to jumps in intact preparations); BSt indicates behaviors observed in brainstem preparations (e.g., BStSwim referring to swims in brainstem preparations); N_BSt indicates the number of synergies for a type of "brainstem" behaviors (e.g., N_BStKK referring to the number of synergies for kicks in brainstem preparations); N_IN means the number of synergies for movements in intact preparations (e.g., N_INWK referring to the number of synergies for walks in intact animals)). For example, in Fig. 12*A*, in intact frog b1, four (N_sh=4) out of five synergies for jumps (N_INJP=5; zero STD, n=20) are similar to synergies for jumps observed in the "brainstem" frog b1 (i.e., after the transection). Comparison of synergies, ***A***, for jumps, ***B***, for swims, ***C***, for kicks, and ***D***, for walks to synergies in the execution of movements observed in brainstem preparations. Note that almost all synergies of four different types of natural motor behaviors remain invariant after transection, suggesting that the brainstem and spinal cord may structure the synergies in the generation of natural motor behaviors in intact animals.

Figure 12 shows that the number of synergies for four different types of natural motor behaviors (N_INJP for jumps; N_INSW for swims; N_INKK for kicks, N_INWK for walks) are close to the number of shared synergies (N_sh), the shared subspace dimensionalities of individual EMG data set recorded during the corresponding movements in intact and brainstem preparations. For example, there were four out of five, four out of four, and three out of three synergies underlying jumps observed both in intact and in brainstem frogs b1, b2, and b3, respectively. This tendency is consistent across all four natural motor behaviors recorded in the study, even though there was interanimal variability in the N_sh, the number of synergies observed in the execution of movements both in intact and in brainstem preparations. Furthermore, note that the difference in the ratio of shared subspace dimensionality (SSD) to the number of brainstem synergies (N_BSt) or the number of intact synergies (N_IN) for swims and walks shown in Figure 13 is due to the smaller number of synergies required to produce swims and walks in brainstem preprarations in frog b1 and b2 (see Fig. 12*B* for swims and Fig. 12*D* for walks). The group analysis in Figure 13 confirms the results explained above: almost all synergies utilized in the execution of natural motor behaviors are preserved after transection, suggesting that the neural circuitries in the brainstem and spinal cord may be involved in programming muscle synergies underlying natural motor behaviors.

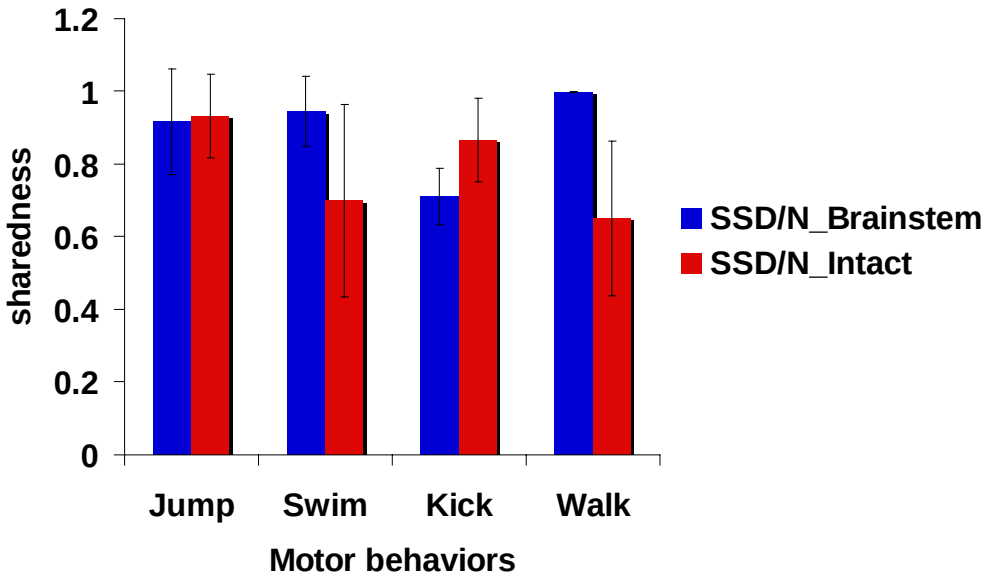

Figure 13. A majority of synergies in intact preparations remains invariant after transection at the level of the caudal end of the third ventricle. Each red bar (mean±STD; n=20) represents the ratio of the shared subspace dimensionality (SSD) to the number of synergies observed in intact preparations (N_IN), indicating to what extent a set of synergies underlying each individual natural motor behavior is similar to synergies explaining motor behaviors in brainstem preparations. Each blue bar (mean±STD; n=20) represents the ratio of SSD to the number of synergies observed in brainstem preparations (N_BSt), indicating to what extent the SSD is constrained by the number of synergies underlying motor behaviors in brainstem preparations. Note that a "sharedness" is over 0.8, over four out of five, illustrating almost all synergies in intact preparations are similar to synergies extracted from EMGs recorded in brainstem preparations.

Reconstructing EMGs recorded during natural motor behaviors by combination of synergies from the step II analysis

If a set of shared and natural movement-specific synergies from the *step II analysis* are sufficient to explain the variance of the original EMGs recorded during natural movements, the set of the synergies should reconstruct individual episodes of natural motor behaviors well. Figure 14 shows that EMG samples during jumps and kicks are reconstructed by a combination of synergies underlying the two behaviors, respectively, observed in frog b2. The reconstruction R^2s for the two examplified episodes are 0.939 and 0.947, respectively. In Figure 15, the reconstruction R^2s across all individual natural motor behaviors recorded in three animals (frog b1, b2, and b3) are above 90%, suggesting that the modified version of the NMF utilized in the *step II analysis* can successfully extract synergies underlying four different major types of motor behaviors of the animals.

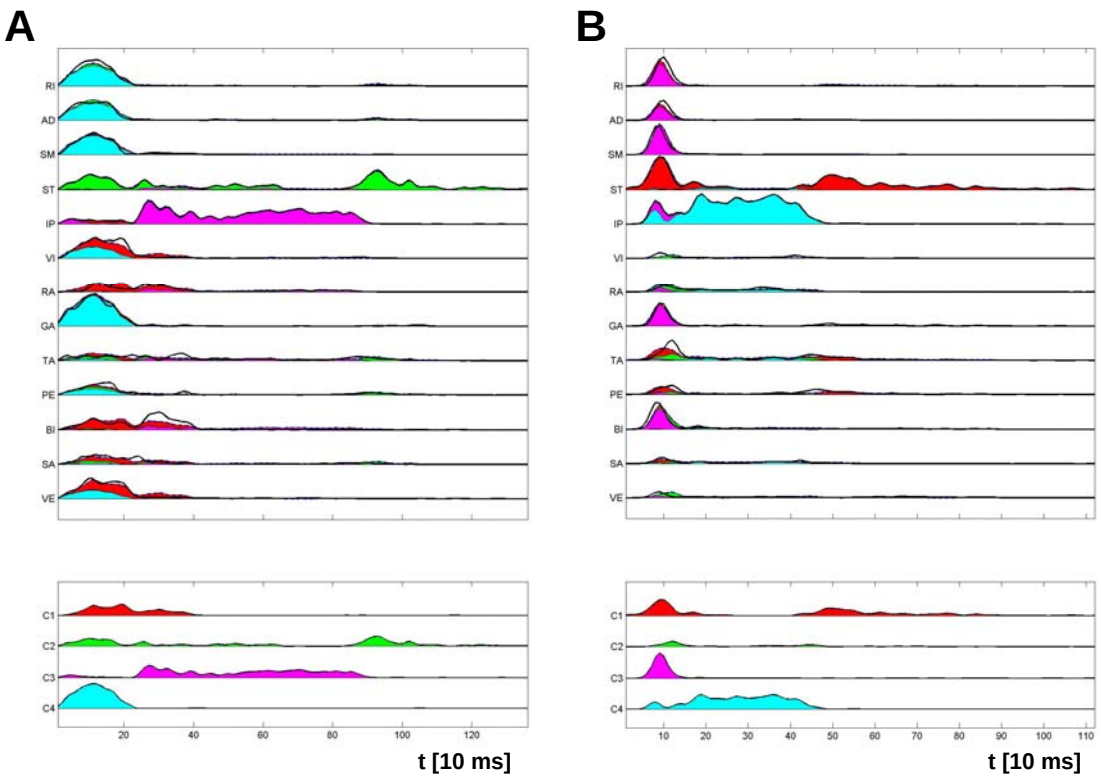

Figure 14. Examples of reconstruction of the muscle patterns recorded during jumping and kicking episodes of frog b2. The averaged, rectified, filtered, and integrated EMGs were reconstructed by combining synergies and their corresponding coefficients (for filtering and integration parameters and full names of muscles, see Materials and Methods). The original data (top panel, thin line and shaded area) are shown as being superimposed onto their reconstruction (thick line) by a combination of the synergies. The colors of the reconstruction (top panel) match the colors of the coefficients (bottom panel) of synergies to indicate how each synergy contributes to reconstruct each data point. ***A***, The original and reconstructed EMGs of an episode of jump. ***B***, The original and reconstructed EMGs of an episode of kick.

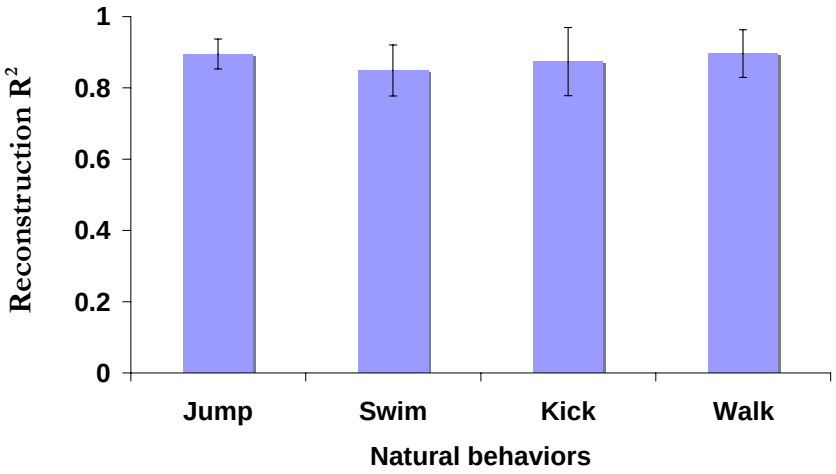

Figure 15. Robustness of synergies in the *stage II analysis* across different individual natural motor behaviors (jumping, swimming, kicking, and walking). R^2 (mean±STD; n=20) represents the fraction of total variation accounted for by combining synergies and their corresponding coefficients. A set of synergies shared between EMGs recorded during movements in intact and brainstem preparations and "intact" EMG data-specific synergies is sufficient to explain over 90% of the data variance of original EMGs recorded during individual natural motor behaviors.

Experiment II. Muscle synergies underlying movements in intact and "medullary" animals

In the previous section, I assessed the similarity of synergies underlying motor behaviors in intact and transected animals. Since brainstem preparations can perform four major types of movements observed in intact frogs, it was possible to directly compare synergies explaining each of four motor behaviors before and after the transection. I then investigated differences between intact and "medullary" preparations (i.e., animals after transection at the level of the caudal end of the pons) to assess the extent of modulation of muscle synergies from the supra-medullary circuitries. As displayed in Figure 4, EMG patterns during movements obtained from the medullary preparation show similarities with the EMG motor pattern recorded during natural motor behaviors with a variability of the duration and amplitude of muscle activation. The findings motivated me to analyze the similarity of synergies in the execution of movements observed before and after the transection.

Observation of the structure of muscle synergies in movements before and after the transection

One major difference between "brainstem" behaviors and "medullary" behaviors is the behavioral repertoire: while the "brainstem" preparations can perform all four major types of natural movements (jumps, swims, kicks, and walks), the medullary preparations can produce only limited kinds of motor behaviors, such as kicks, walks (steps), and reflexes.

In Figures 16 and 17, I display synergies of four different types of movements observed in frog m3 before and after transection. Each synergy from the intact animal was reordered and was matched with each synergy observed in the medullary preparation (the best-matching scalar product). Figs. 16*A* and 16*B* demonstrate a set of four synergies in the intact frog during jumps and a set of seven synergies observed during jumps in the medullary preparation. In Fig. 16*A*, the first two jump synergies appear similar to the synergies of the "medullary" preparation.

In Fig. 16*C*, the first four synergies underlie movements observed both in the intact and in the medullary preparation: (1) ST, a hip extensor and a knee flexor-dominant one, (2) AD, a hip extensor-dominant one, (3) TA, a knee extensor and an ankle flexor-dominant one, and (4) hip flexors, knee extensors (VE and VI), and an ankle flexor-activated one, respectively. The fifth intact swim synergy is dominated by GA, a knee flexor and an ankle extensor. Thus,

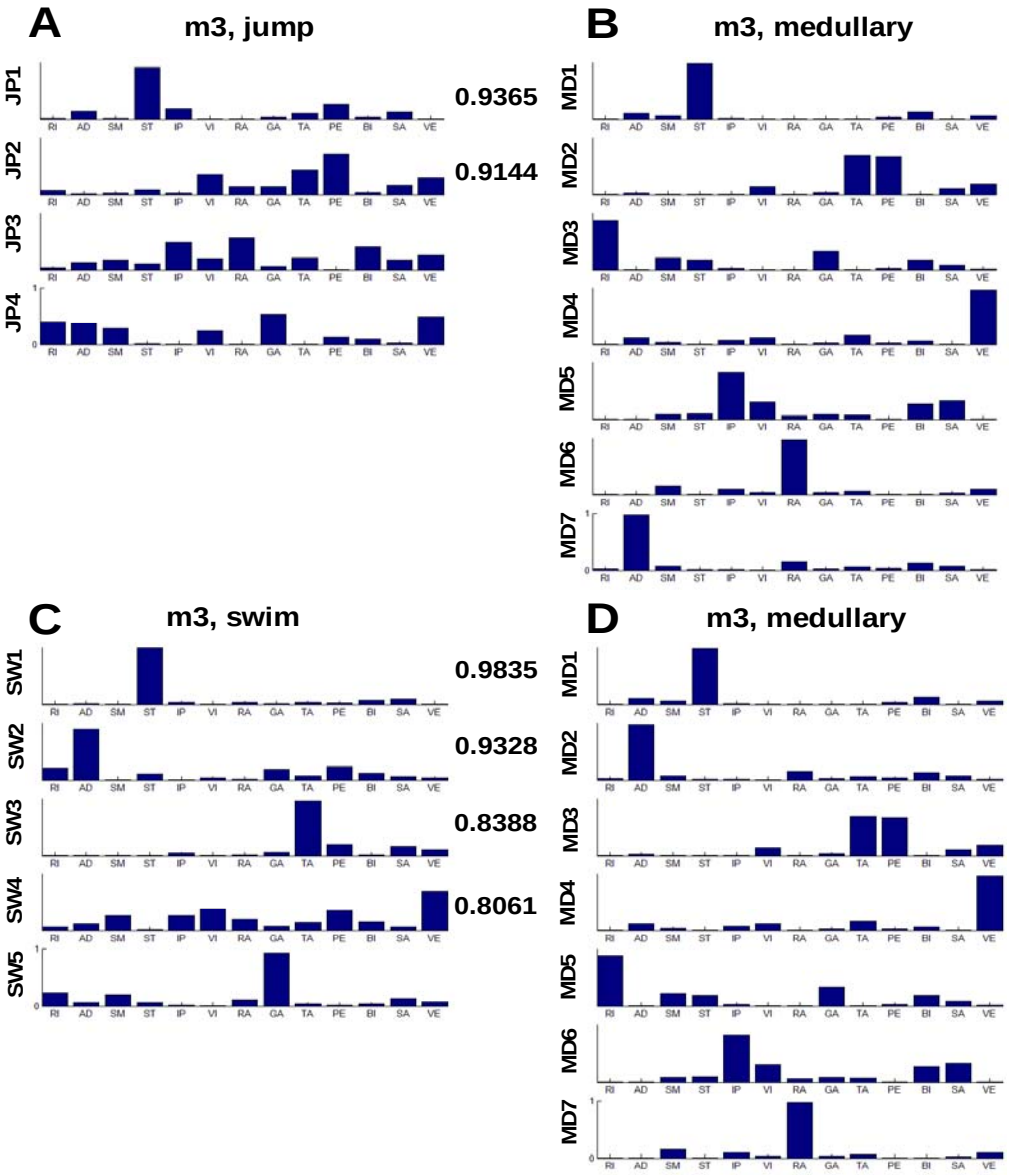

Figure 16. Examples of synergies extracted separately from each behavioral EMG data set during jumping, swimming, and medullary motor behaviors of frog m3. The first two of four (Fig. 16*A*) or the first four of five (Fig. 16*C*) synergies for natural movements are matched to the corresponding number of the synergies for medullary movements (Figs. 16*B* and 16*D*), which make the best-matching scalar product. The numbers between the two synergies are the statistically significant scalar products (p<0.05), demonstrating how similar two synergies are. The comparison of synergies ***A*** and ***B***, for natural jumps and medullary movements and, ***C*** and ***D***, for natural swims and medullary movements.

the structure and the corresponding function of muscle synergies of jumps and swims before and after the transection are more or less similar with a minute variability of balance of muscle activation.

The first four kick synergies in Fig. 17*A* are similar in the structure of the first four medullary kick synergies: (1) ST, a hip extensor and a knee flexor-dominant synergy, (2) RI and GA, a hip extensor, knee flexor, and an ankle extensor-dominant one, (3) IP, a hip flexor-dominant one, and (4) VE, VI, and TA, hip flexors, knee extensors, and an ankle flexor-dominant one, respectively. While the fifth (hip extensors and knee flexors-dominant) and sixth (a knee extensor and an ankle flexor-dominant) intact kick synergy do not have a corresponding one with similar structure among synergies in the medullary preparation, their functional counter-synergies (MD2 and MD7) exist, respectively. Similarly, in Fig. 17*C*, the first four synergies for walks recorded in the intact animal appear as synergies for walks in the medullary preparation: (1) VE, a hip flexor and a knee extensor-dominant synergy, (2) ST, a hip extensor and a knee flexor-dominant one, (3) IP, a hip flexor-dominant one, and (4) PE and TA, knee extensors and ankle flexors-dominant one, respectively. In summary, by visual inspection, a large portion of muscle synergies before and after the transection are almost identical with some variability in the structure of synergies and function of muscles activated in each synergy.

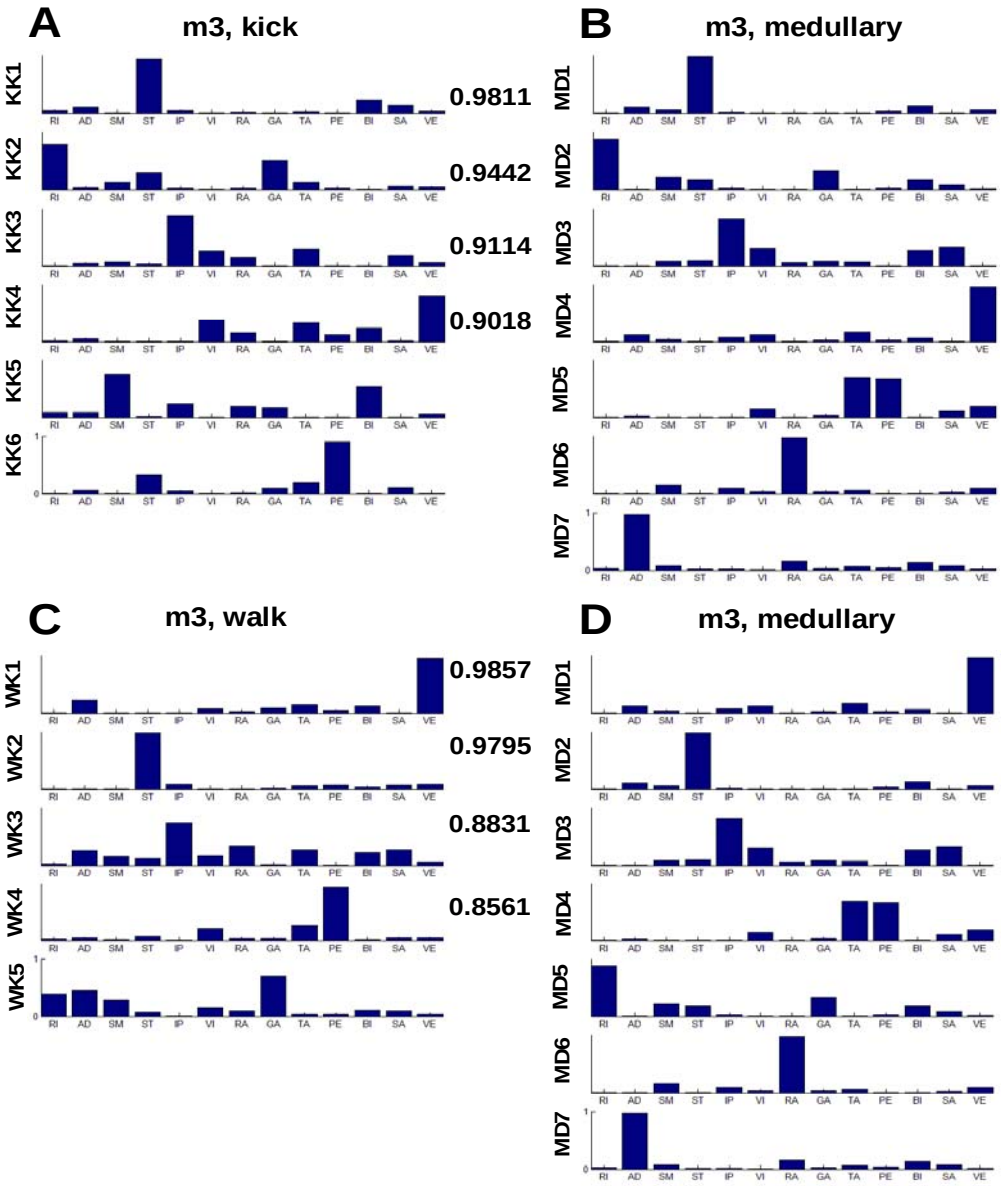

Figure 17. Examples of synergies extracted separately from each behavioral EMG data set during kicking, walking, and medullary motor behaviors of frog m3. The first four of six (Fig. 17*A*) or the first four of five (Fig. 17*C*) synergies for natural movements are matched to the corresponding number of the synergies for medullary movement (Figs. 17*B* and 17*D*), which make the best-matching scalar product. The numbers between the two synergies are the statistically significant scalar products ($p<0.05$), demonstrating how similar two synergies are. The comparison of synergies ***A*** and ***B***, for kicks in the intact animal and "medullary" movements, ***C*** and ***D***, for walks in the intact animal and "medullary" movements.

Analysis in step I: estimating similarity of muscle synergies

As in the first set of experiments (the ***intact vs. brainstem*** condition), two quantitative measures were computed to calculate how similar synergies are before and after the transection: i.e., I computed (1) the number of shared synergies (NSS) and (2) the shared subspace dimensionality (SSD) (Cheung et al., 2005).

In Figures 16 and 17, the results of scalar products that were statistically significant ($p<0.05$) are shown between the two sets of synergies in frog m3. The number of best-matching scalar products are quantified as the NSS, and the summary of the numbers is shown in Table 3.

Table 3. Summary of *stage I analysis*: estimating the number of synergies shared between the synergy sets in intact and "medullary" preparations

Frog	Comparison Condition	N_{IN}	N_{MD}	NSS	SSD	Similarity	Subangle	R^2 (%)	
								Intact	Medullary
m1	Jump vs Medullary	5±0	7±0	3.668±0.527	3.955±0.208	0.931±0.052	0.178±0.149	0.923±0.003	0.919±0.004
m2	Jump vs Medullary	4±0	6±0	1.678±0.468	2.000±0.000	0.847±0.024	0.217±0.083	0.920±0.000	0.928±0.000
m3	Jump vs Medullary	4±0	7±0	2.673±0.756	2.855±0.353	0.870±0.050	0.209±0.124	0.907±0.002	0.918±0.000
m1	Swim vs Medullary	5±0	7±0	3.100±0.300	3.155±0.362	0.974±0.029	0.086±0.074	0.917±0.000	0.919±0.004
m2	Swim vs Medullary	5±0	6±0	4.455±0.707	3.528±0.539	0.884±0.071	0.232±0.107	0.910±0.001	0.928±0.000
m3	Swim vs Medullary	5±0	7±0	3.660±0.474	3.000±0.000	0.889±0.070	0.135±0.103	0.917±0.000	0.918±0.000
m1	Kick vs Medullary	4±0	7±0	2.678±0.479	3.000±0.000	0.910±0.058	0.193±0.142	0.925±0.000	0.919±0.004
m2	Kick vs Medullary	5±0	6±0	2.230±0.647	1.843±0.365	0.796±0.028	0.390±0.039	0.904±0.000	0.928±0.000
m3	Kick vs Medullary	6±0	7±0	4.300±0.464	3.085±0.279	0.904±0.059	0.149±0.114	0.912±0.001	0.918±0.000
m2	Walk vs Medullary	5±0	6±0	1.858±0.590	2.650±0.478	0.908±0.070	0.178±0.120	0.924±0.000	0.928±0.000
m3	Walk vs Medullary	5±0	7±0	3.625±0.617	3.000±0.000	0.924±0.060	0.105±0.044	0.918±0.003	0.918±0.000

Two parameters (NSS, number of shared synergies; SSD, shared subspace dimensionality) are used to estimate the number of common synergies between movements observed in intact and medullary preparations (N_{IN}, number of "intact" synergies, N_{MD}, number of "medullary" synergies; all values are mean±STD; n=20).

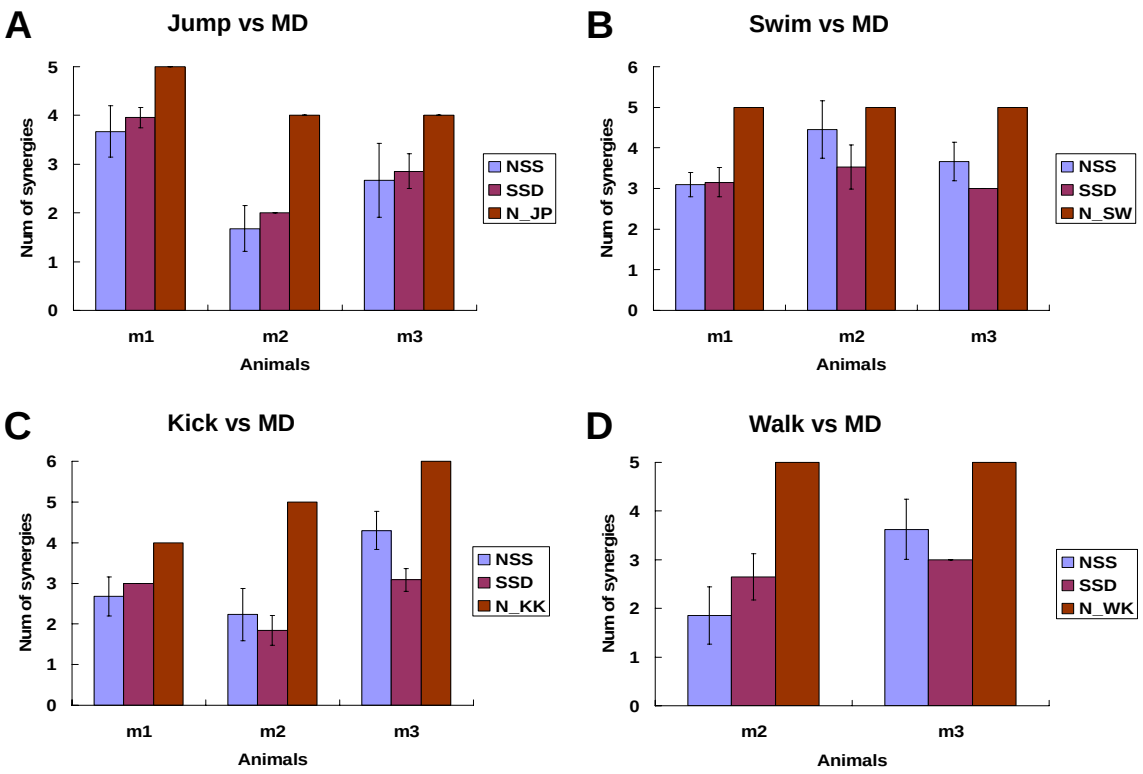

Figure 18. A large portion of synergies for individual natural motor behaviors remain invariant after transection at the level of the caudal pons (MD, movements in "medullary" preparations; NSS, number of shared synergies; SSD, shared subspace dimensionality; N_JP, number of synergies for jumps; N_SW, number of synergies for swims; N_KK, number of synergies for kicks; N_WK, number of synergies for walks). NSS and SSD are two quantitative parameters indicating how many synergies are common in movements observed in intact and "medullary" preparations. For example, in Fig. 18*A*, in frog m1, about four out of five synergies for jumps (mean±STD, n=20) are similar to synergies for "medullary" motor behaviors (NSS), and about four out of five subspace dimensionalities for dataset recorded during jumps (mean±STD, n=20) are similar to dimensionalities of subspaces spanned by a set of synergies in medullary preparations (SSD). Comparisons of synergies, ***A***, for jumps and "medullary" movements, ***B***, for swims and "medullary" movements, ***C***, for kicks and "medullary" movemnts, and ***D***, for walks and "medullary" movements. Note that there is interanimal variability in terms of NSS and SSD across all four (***A***, ***B***, ***C***, and ***D***) comparisons.

Furthermore, the degree of overlap between the subspaces spanned by the sets of synergies utilized in the execution of movements in intact animals and synergies observed in medullary preparations (SSD) was calculated by computing principal angles (Golub and van Loan, 1983). Figure 18 shows the SSD between the synergeis in intact and medullary preparations (Fig. *18A*, synergies for jumps and "medullary" movements; Fig. *18B*, synergies for swims and medullary movements; Fig. *18C*, synergies for kicks and medullary movements; and Fig. *18D*, synergies for walks and medullary movements) across all animals from which EMG data were recorded. On average, four out of five, two out of four, and three out of four dimensions of the subspaces spanned by the synergies in jumps in intact frog m1, m2, and m3, respectively, are shared with their corresponding subspaces spanned by synergies in "medullary" EMG data. Three out of five, four out of five, four out of five dimensions of the subspaces spanned by a set of synergies underlying swims in all three intact animals are shared with the subspaces spanned by synergies for medullary movements. For kicks, three out of four, two out of five, three out of six dimensions of the subspaces spanned by sets of synergies in intact animals intersect with the dimensionalities of subspaces spanned by "medullary" synergies. Similarly, in walks, three of five and three of five dimensionalities are overlapped with dimensionalities of subspaces spanned by "medullary" synergies. Note that, even though the subspaces of intact and medullary synergies are not identical (i.e., completely overlapping with each other), NMF successfully found synergies for four major types of frog behaviors (jumping, swimming, kicking, and walking), which span shared subspaces before and after transection. The summary of *stage I analysis* is shown in Table 3.

Figure 19 shows that sharedness, the ratio of the number of common synergies to the total number of synergies for the four individual natural motor behaviors, is significant, suggesting that modulation of the muscle synergies underlying natural motor behaviors from supra-medullary circuitries is minor. These results support the idea that the neural circuitries localized in the medulla and spinal cord are sufficient to program key elements of muscle synergies utilized in the execution of natural movements.

In *stage I analysis*, synergies were extracted separately from the data sets recorded from intact and "medullary" preparations, and there are possible shortcomings of the separate extraction method (see Materials and Methods). Thus, I performed the second step of analysis.

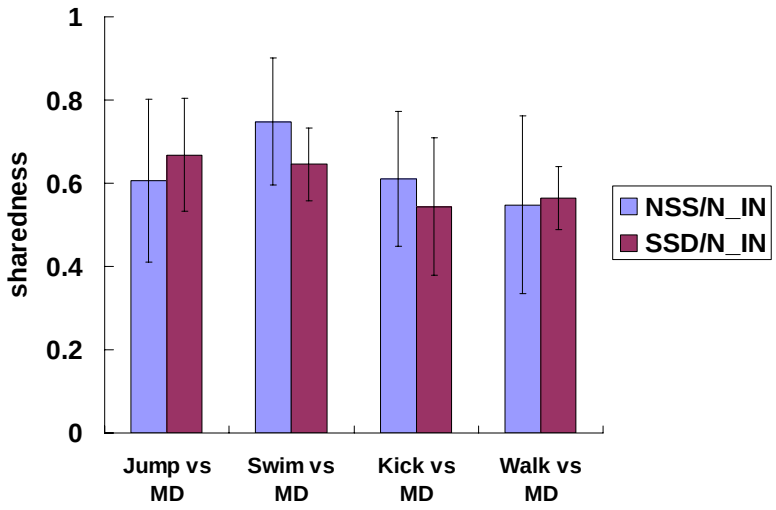

Figure 19. Ratios of the number of shared synergies to the total number of synergies for individual natural motor behaviors across four different comparison conditions. Sharedness represented in the y-axis indicates the ratio of the number of shared synergies (NSS) or the shared subspace dimensionality (SSD) to the number of synergies for each natural motor behavior (N_IN) from all animals recorded. All light blue bars indicate the ratio of NSS to N_IN, while all purple bars refer to the ratio of SSD to N_IN. Across all four comparisons of natural and "medullary" motor behaviors, over 60% of synergies observed in intact animals remain invariant after transection at the level of the caudal end of the pons. The results suggest that the neural circuitries in the medulla and spinal cord may be sufficient to program muscle synergies utilized in the execution of motor behaviors in intact animals (JP, jumping; MD, medullary motor behavior; SW, swimming; KK, kicking; WK, walking).

Analysis in step II: extracting shared and EMG data set-specific synergies

In this *stage II analysis*, I utilized the modified version of the NMF (Cheung et al., 2005) to extract two types of synergies from the concatenated data recorded in intact and "medullary" preparations: shared synergies between the two data sets and single data set-specific synergies.

Figure 20 demonstrates examples of how I estimated the number of synergies common in both EMG data sets recorded before and after transection. In *stage II analysis*, as performed in Experiment I section (the ***intact vs. brainstem*** condition), the appropriate numbers of shared synergies were determined when the remaining shared dimensionality between "intact" and "medullary" EMG data sets became less than a threshold of 0.25 as the number of shared synergies increased. For instance, in Figs. 20*A*-20*D*, when four of five, five of six, four of six, and four of five shared synergies were extracted, respectively, the remaining shared dimensionality between individual "intact" EMG data-specific and "medullary" EMG data-specific synergies decreased below 0.25, a threshold. This indicates that there are four out of five, five out of six, four out of six, and four out of five synergies underlying both EMG data sets recorded during the individual natural and "medullary" behaviors.

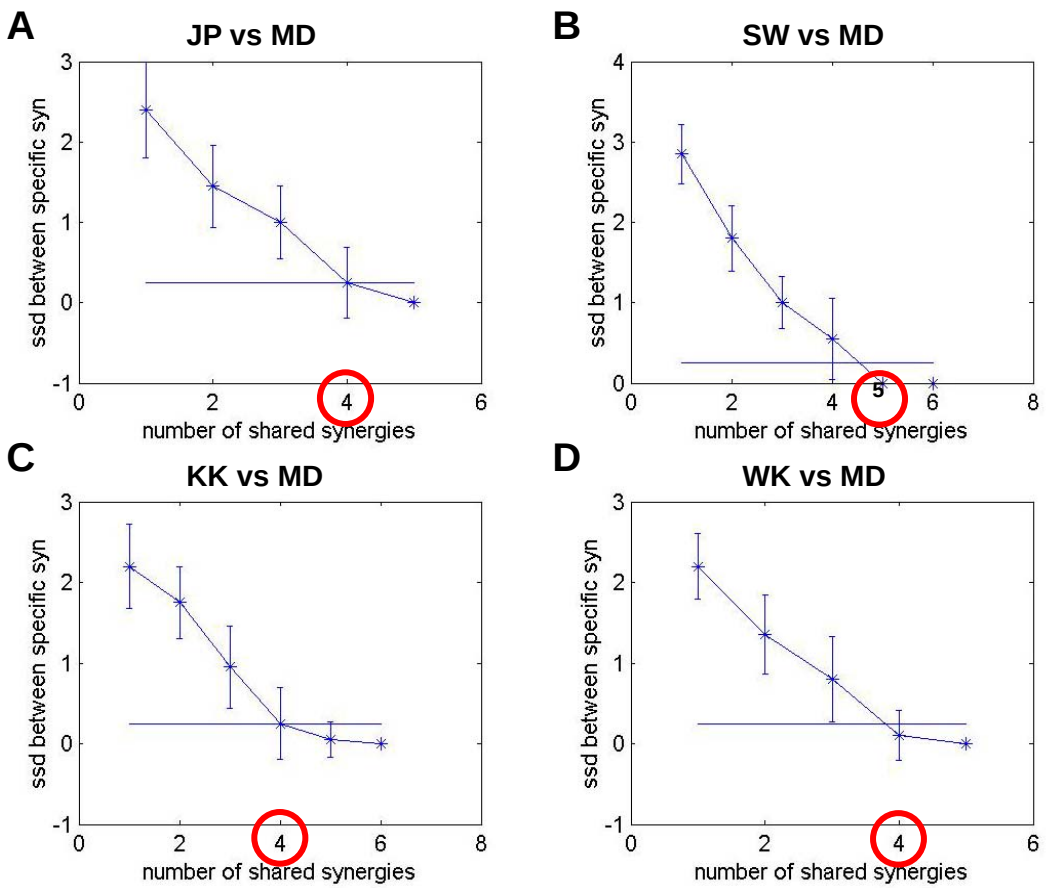

Figure 20. Estimating the number of shared synergies in the *analysis stage II*. As the number of shared synergies (N^{sh}) increases progressively, the dimensionality of the subspace shared between the specific synergies (ssd) for natural and "medullary" behaviors decreases. Estimating the correct number of shared synergies was done by finding the number of shared synergies at which the specific synergies no longer share a common subspace; that is, at the maximum N^{sh}, the shared dimensionality was defined to be zero. Here the correct N^{sh} was selected as the smallest N^{sh} with a shared dimensionality falling below 0.25. In each subplot (***A***, ***B***, ***C***, and ***D***), the mean shared dimensionality between the specific synergies (mean±SD; n=20) is circled in red. ***A***, Four out of five synergies for jumps, ***B***, five out of six synergies for swims, ***C***, four out of six synergies for kicks, and ***D***, four out of five synergies for walks are similar to synergies structured by the neural circuitries within the medulla and spinal cord.

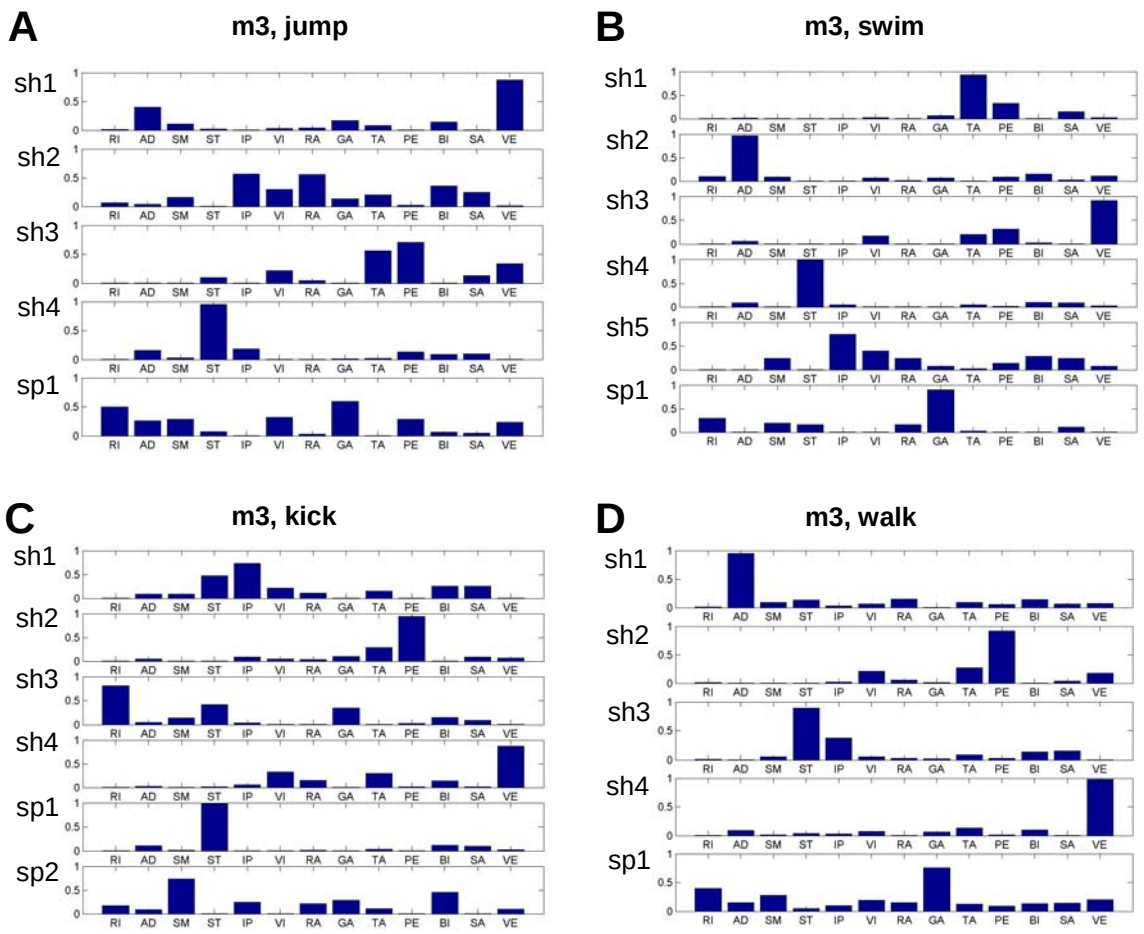

Figure 21. Sets of synergies extracted from the EMGs during four individual natural behaviors of frog m3 in the *analysis stage II*. Each synergy represents the balance of activation of muscles recorded. The full terms of the abbreviated muscle names are shown in Materials and Methods. ***A***, A set of four shared (first four) and one "medullary" EMG data-specific synergies for jumps. ***B***, A set of five shared (first five) and one "medullary" EMG data-specific synergies for swims. ***C***, A set of four shared (first four) and two "medulalry" EMG data-specific synergies for kicks. ***D***, A set of four shared (first four) and one "medullary" EMG data-specific synergies for walks.

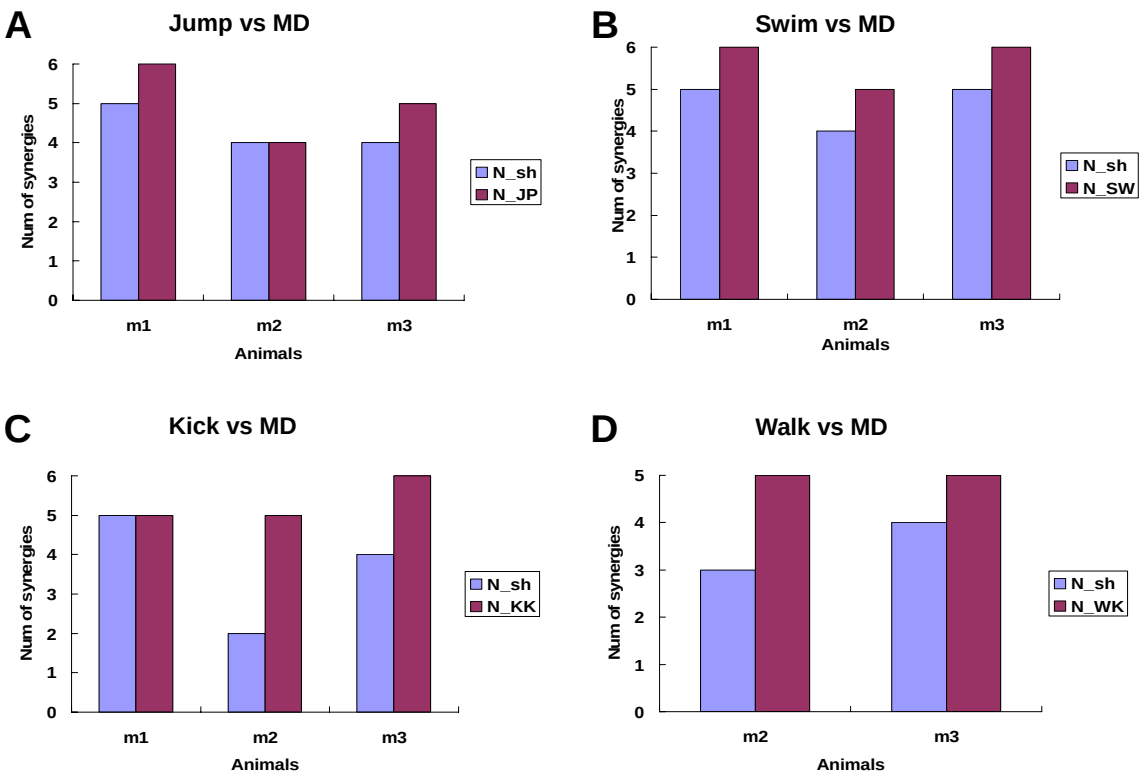

Figure 22. The number of shared synergies (N_sh) and the number of synergies for individual natural motor behaviors in the *analysis stage II*. Each subplot (***A***, ***B***, ***C***, or ***D***) demonstrates that almost all synergies in the execution of individual natural motor behaviors remain invariant in "medullary" preparations (MD, medullary; N_sh, number of shared synergies; N_JP, number of synergies for jumps; N_SW, number of synergies for swims; N_KK, number of synergies for kicks; N_WK, number of synergies for walks). For example, in Fig. 22*A*, five (N_sh=5) out of six synergies (N_JP=6; zero STD, *n*=20), four (N_sh=4) out of four synergies, and four (N_sh=4) of five synergies, in three animals (frog m1, m2, and m3, respectively), during jumps are similar to synergies for "medullary" motor behaviors. Comparison of synergies, ***A***, for jumps, ***B***, for swims, ***C***, for kicks, and ***D***, for walks to synergies in the execution of movements in medullary preparations. Note that almost all synergies of four different types of natural behaviors appear as the synergies for movements in medullary preparations with an interanimal variability.

The same methods described above were applied to data collected from all frogs, and Figure 21 illustrates representative examples of synergy sets for jumps, swims, kicks, and walks in *stage II analyses*. Intriguingly, the synergies extracted at the *stage II analysis* are all matched to those at the *stage I analysis*, in the set of experiments the ***intact vs. medullary*** condition. For instance, in Fig. 21*A*, sh1 to sh4 synergies (i.e., synergies underlying both jumps in intact animals and "medullary" movements) and sp1 synergy (i.e., a synergy underlying only medullary movements but not jumps in intact animals) are similar to JP4, JP3, JP2, JP1, and JP4, respectively, in Fig. 16*A*; in Fig. 21*B*, sh1 to sh5 and sp1 synergies are similar to SW3, SW2, SW4, SW1, MD6, and SW5, respectively, in Figs. 16*C* and 16*D*. Similarly, in Fig. 21*C*, sh1 to sh4 and sp1 to sp2 synergies are close to KK3, KK6, KK2, KK4, KK1, and KK5, respectively, in Fig. 17*A*; in Fig. 21*D*, sh1 to sh4 and sp1 are close to MD7, WK4, WK2+WK3, WK1, and WK5, respectively, in Figs. 17*C* and 17*D*. The summary of the *stage II analyses* across all three animals is shown in Table 4.

Figure 22 shows that the number of synergies for four different types of movements observed in intact preparations (N_JP for jumps; N_SW for swims; N_KK for kicks; and N_WK for walks) are close to the number of shared synergies (N_sh), the shared subspace dimensionalities of movements performed by intact and "medullary" preparations. For example, as shown in Fig. 22*A*, five out of six, four out of four, and four out of five dimensionalities of subspaces spanned by synergies explaining EMGs recorded during both natural jumps and "medullary" movements of the frog m1, m2, and m3, respectively. This tendency is consistent across all four natural behaviors recorded in the study, with interanimal variability in the N_sh, the number of common, "shared" synergies for both natural and "medullary" movements. The group analysis in Figure 23 confirms the results explained above: almost all synergies utilized in the execution of individual natural motor behaviors are preserved in the execution of movements after the transection at the level of the caudal end of the pons, suggesting that the neural circuitries in the medulla and spinal cord may program key elements of muscle synergies underlying natural motor behaviors.

Table 4. Summary of *stage II analysis*: estimating the number of synergies shared between the "intact" and "medullary" EMG data sets

Frog	Comparison Condition	N_{IN}	N_{MD}	N_{sh}	N_{sp_IN}	N_{sp_MD}	R^2 (%)	
							Intact	Medullary
m1	Jump vs Medullary	5	7	5	0	2	0.889±0.015	0.900±0.004
m2	Jump vs Medullary	4	7	4	0	3	0.918±0.001	0.857±0.005
m3	Jump vs Medullary	5	7	4	1	3	0.927±0.005	0.886±0.008
m1	Swim vs Medullary	6	7	5	1	2	0.897±0.015	0.917±0.005
m2	Swim vs Medullary	5	6	4	1	2	0.888±0.010	0.927±0.001
m3	Swim vs Medullary	6	7	5	1	2	0.911±0.011	0.905±0.006
m1	Kick vs Medullary	5	7	5	0	2	0.876±0.033	0.899±0.009
m2	Kick vs Medullary	5	6	2	3	4	0.892±0.008	0.893±0.014
m3	Kick vs Medullary	6	7	4	2	3	0.903±0.007	0.914±0.007
m2	Walk vs Medullary	5	6	3	2	3	0.909±0.008	0.921±0.006
m3	Walk vs Medullary	5	7	4	1	3	0.899±0.005	0.910±0.005

See Materials and Methods for details on how to extract synergies in *stage II analysis* (N_{IN}, number of "intact" synergies; N_{MD}, number of "medullary" synergies; N_{sh}, number of shared synergies; N_{sp_IN}, number of "intact" data-specific synergies; N_{sp_MD}, number of "medullary" data-specific synergies; R^2, percentage of data variance explained by a combination of the listed numbers of synergies; all values are mean±STD; no STD indication means zero STD; n=20).

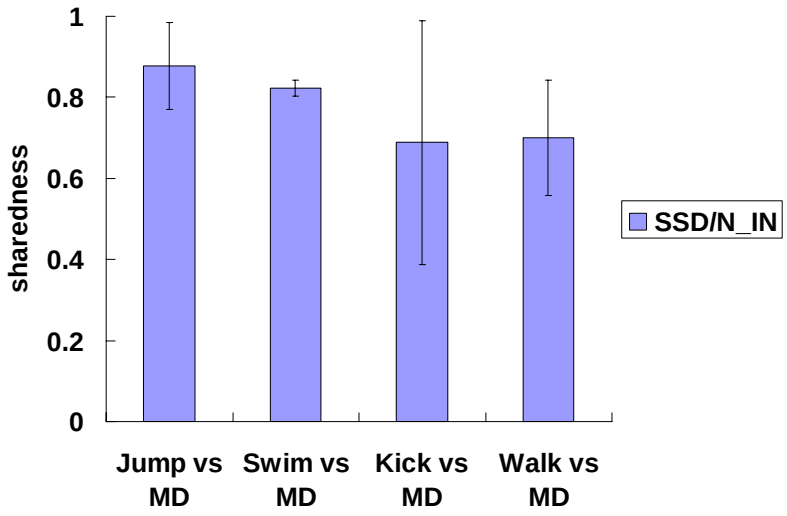

Figure 23. A majority of synergies underlying movements observed in intact preparations remains invariant after transection in medullary preparations. Each light blue bar (mean±STD; n=20) represents "sharedness", the ratio of the shared subspace dimensionalities (SSD) to the number of synergies in intact preparations (N_IN), indicating the degree of modulation of muscle synergies from the supra-medullary circuitries. Note that the sharedness is 0.8, four out of five, illustrating almost all synergies in intact preparations are similar to synergies in the execution of medullary motor behaviors.

Reconstructing EMGs recorded during natural motor behaviors by combination of synergies from the step II analysis

Figure 24 shows that EMG samples during swimming and walking are reconstructed by a combination of synergies underlying the two motor behaviors, respectively, of frog m3. The reconstruction R^2s for the two examplified episodes are 0.939 and 0.947, respectively. In Figure 25, the reconstruction R^2s across all individual natural motor behaviors recorded in the three animals are above 90%, suggesting that the modified version of the NMF utilized in the *step II analysis* can successfully extract synergies underlying four different major types of motor behaviors of the animal.

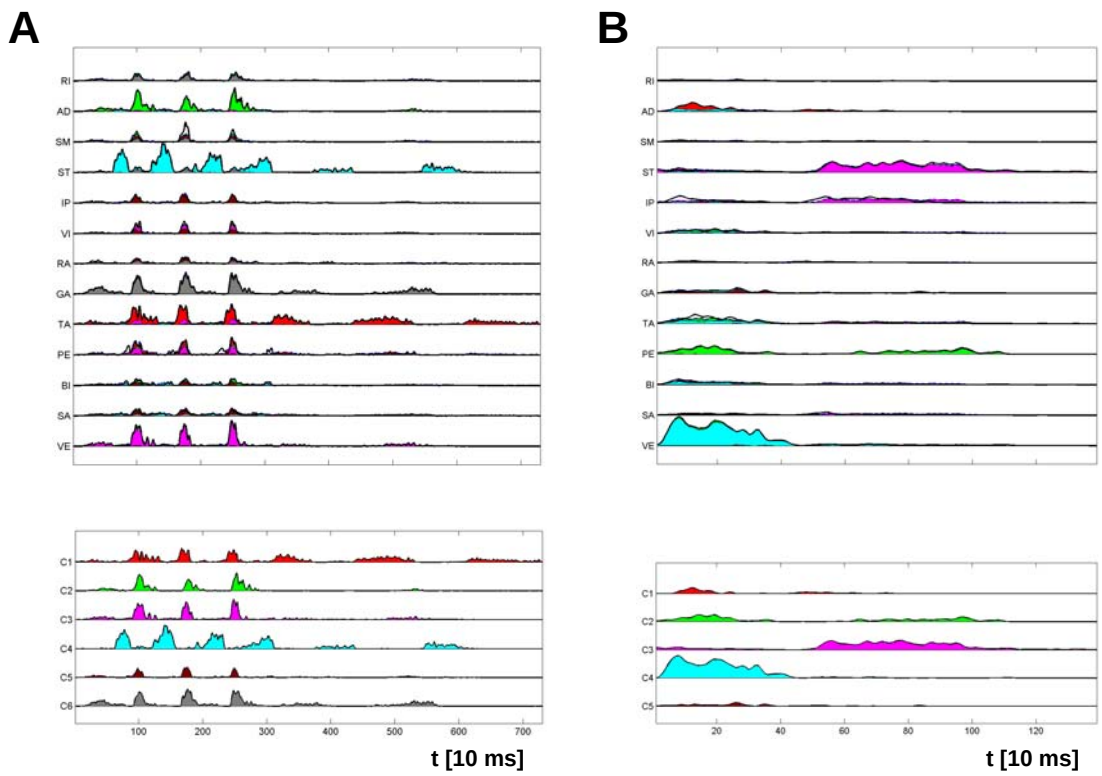

Figure 24. Examples of reconstruction of the muscle activation patterns during swimming and walking episodes of frog m3. The averaged, rectified, filtered, and integrated EMGs (for filtering and integration parameters and full names of muscles, see Materials and Methods) were reconstructed by combining synergies and their corresponding coefficients. The original data (top panel, thin line and shaded area) are shown as being superimposed onto their reconstruction (thick line) by combination of the synergies. The colors of the reconstruction (top panel) match the colors of the coefficients (bottom panel) of synergies to indicate how each synergy contributes to reconstruct each data point. ***A***, The original and reconstructed EMGs of three consecutive swimming cycles. ***B***, The original and reconstructed EMGs of a walking episode.

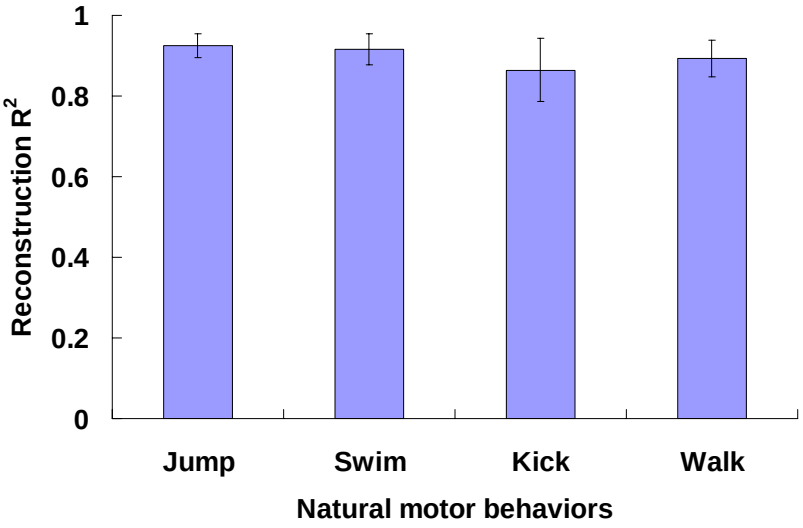

Figure 25. Robustness of synergies in the *stage II analysis* across different individual natural motor behaviors (jumping, swimming, kicking, and walking). R^2 (mean±STD; n=20) represents the fraction of total variation accounted for by combining synergies and their corresponding coefficients. A set of synergies shared between EMGs recorded during individual natural and "medullary" movements and "intact" EMG data-specific synergies is sufficient to explain over 90% of the data variance of original EMGs recorded during individual natural motor behaviors.

Chapter 3

Conclusion

The central nervous system and the musculoskeletal architecture of animals cooperate to generate purposeful, well-coordinated motor acts and movements. This thesis hypothesizes that the motor systems are hierarchically organized and the motor acts and movements are orchestrated in a modular fashion. The thesis has addressed the following questions: (1) whether the neural network within the brainstem and spinal cord are responsible for structuring and combining muscle synergies, in order to generate natural motor behaviors, and (2) whether the neural circuitries within the medulla and spinal cord structure the repertoire of muscle synergies for natural movements.

Combining muscle synergies in the execution of natural movements

To investigate which areas of the central nervous system are necessary and sufficient to combine muscle synergies in movement execution, EMGs during four different types of movements (jumps, swims, kicks, and walks) were recorded. The details of movements are reproducible from animal to animal. In addition, the types of movements studied in this thesis display an extremely wide-spread synergy incorporating the whole musculature and the entire moving skeleton and bringing into play a large number of areas and conduction pathways of the central nervous system (Bernstein, 1967). The movements also display typical and stable structures with adaptive variations in the workspace of animals. In light of all these characteristics of the movements, the four kinds of motor behaviors recorded in experiments were appropriate to investigate the general physiology of movements. This thesis maximizes the data variability by observing all four behaviors in experiments.

The thesis has investigated potentially minimal neuronal divisions that could generate the repertoire of movements observed in intact, freely moving animals. To do this, the animals were transected at the varied level and the motor behaviors were evoked from the reduced animal preparation. When the brainstem was disconnected from the supra-brainstem circuits but kept intact and connected to the caudal region of the brainstem, all four different major types of motor behaviors could be evoked. In addition, the sequence of muscle activation before and after the transection at the level of the caudal end of the third ventricle remained invariant. However, when the transection was at the level of rostral medulla, only a subset of movement repertoire (e.g., kicks and steps) could be evoked. These results suggest that the brainstem and spinal cord, the neuronal areas kept intact after the transection at the level of the caudal end of the third ventricle, are necessary and sufficient to combine the muscle

synergies required in execution of natural motor acts.

In order to test whether the cerebellum is involved in increasing the repertoire of movements observed in reduced preparations, the movements were evoked after transection at the level of the rostral end of the deep cerebellar nuclei to keep the cerebellar structure and the caudal neural divisions of the cerebellum intact. The repertoire of movements observed in this preparation was the same as the repertoire found in the medullary preparations (i.e., mainly kicks and walks, no swims and no jumps). The results may be due to the anatomical fact that the area of the cerebellum in the bullfrog is about 2% of the whole brain area (Nieuwenguys and Donkelaar, 1998). In addition, the results are consistent with the finding of previous studies, in the sense that the cerebellum-damaged animals could produce the reduced repertoire of mfdovements similar to natural movements; cerebellectomy in *Rana fusca* produced only mild alteration of muscle tone and slight ataxia. In the tree frog, *Hyla arborea*, however, cerebellar damage produced marked changes in posture and locomotion (Lutterotti, 1934).

Neural Encoding of muscle synergies

This thesis has compared muscle synergies underlying behaviors recorded from intact and "medullary" preparations (i.e., animals with transection at the level of the caudal end of the pons and with the intact medulla and spinal cord). In the medullary animals, the medulla and spinal cord, the neuronal areas dissociated from the supra-medullary circuitries and kept intact after the transection, are assumed to generate motor behaviors. The NMF analysis of the EMGs from medullary preparations showed that the medullary motor behaviors are composed of a small number of muscle synergies that reflect basic aspects of muscle activation patterns structured by the medullary and spinal circuitries. In addition, the dimensionality of the medullary movements is similar to that of natural movements recorded before the transection. Interestingly, muscle synergies underlying natural movements remain invariant after the transection, in terms of the dimensionality of subspaces spanned by the set of muscle synergies for different movements. The results support the idea that the supra-medullary circuitries do not significantly modulate the structure of muscle synergies structured by the neural circuitries of the medulla and spinal cord. Overall, all findings suggest that the medulla and spinal cord are involved in structuring the muscle synergies underlying natural motor behaviors.

EMGs recorded during movements of spinalized frogs were also recorded (not shown in the thesis). The spinal motor behaviors observed in experiments with spinal preparations were mainly spinal reflexes and the dimensionality of EMGs during the spinal reflexes (three or four) was smaller than that during natural movements (four to six). In addition to the smaller dimensionality of EMGs, the EMG data from spinal animals are limited by the limited repertoire of movements. As a result, a fair comparison between these data and EMG data from intact animals is not possible. We, therefore, intentionally omitted the procedure to compare natural and spinal movements at the level of motor primitives in this thesis.

There have been a variety of data that support the spinal encoding of motor modules in a range of animals (Jankowska et al., 1967a, b; Engberg and lundberg, 1969; Grillner, 1981; Mortin et al., 1985; Robertson et al., 1985; Bizzi et al., 1991; Giszter et al., 1993; Grillner et al., 1995; Stein et al., 1995; Cheng et al., 1998; Roberts et al., 1998; Saltiel et al., 1998; Tresch and Bizzi, 1999; Giszter and Kargo, 2000; Kargo and Giszter, 2000a; Kargo and Giszter, 2000b; Saltiel et al., 2001; Tresch et al., 2002; d'Avella et al., 2003; d'Avella and Bizzi, 2005; Saltiel et al., 2005). However, there have been no studies that demonstrate whether the motor modules observed in a range of natural movements are structured by the spinal cord and its heavily connected neural circuitries. This was the direct motivation of the current thesis: to assess the extent of modulation of muscle synergies observed in medullary preparations from the supra-medullary networks.

Significant synergy sharing before and after transection at various levels

The majority of muscle synergies underlying natural movements remain invariant after transection leaving the brainstem and spinal cord connected. In addition, the structure of almost all muscle synergies explaining natural motor behaviors did not change after transection disconnecting the medulla and supra-medullary structures and keeping the medulla and spinal cord connected and intact. The results support the idea that supra-medullary circuitries are not involved in modulating the structure of muscle synergies encoded within the neural circuitries of the medulla and spinal cord.

The reasons that the modules of all four different types of natural movements were found to be similar to modules of "medullary" movements (i.e., movements recorded after transection at the level of rostral medulla) may be as follows. First, the dimensionalities of medullary movements (six to seven) are higher than that of natural movements (mostly four

to six). Second, the brainstem is known to send inhibitory projections to the spinal cord to produce well-coordinated movements, but the supra-medullary circuitries are disconnected from the medulla in the medullary preparations. Thus, I speculate that (1) the lack of appropriate inhibitory descending commands may be responsible for combining excessive, unnecessary muscle synergies in the execution of medullary movements, and (2) the muscle synergies found in medullary movements are among the large repertoire of muscle synergies structured by the medulla and spinal cord.

Furthermore, as I observed in the given study as well, similar synergies are used in the execution of multiple natural motor behaviors (d'Avella and Bizzi, 2005). That is, a subset of muscle synergies underlying the medullary movements are partially shared with the set of muscle synergies necessary to generate each individual natural motor behavior.

Even though many muscle synergies subserving four different types of natural movements remain invariant after transection at the level of the caudal end of the third ventricle (in brainstem preparations) or the pons (in medullary preparations), it is clear that there exist behavior-specific synergies. For example, as shown in Figures 2, 3, and 4, the disconnection of remaining neuronal circuitries in the animal preparation from the supra-brainstem or supra-medullary circuitries causes changes in the resulting EMG activation recorded during movements after the corresponding transection. Such alterations in burst duration and amplitude of EMGs have been consistently found in other studies (Happee, 1993; Hoffman and Strick, 1993; Schotland and Rymer, 1993; Gottlieb, 1996; Mackey et al., 2002; Saltiel and Rossignol, 2004; Cheung et al., 2005). Therefore, the supra-brainstem or supra-medullary circuitries may take part in movement execution, but not in a way to change the structure of muscle synergies.

Since the majority of muscle synergies remain constant before and after a surgical transection and the muscle model utilized in this thesis enforces to explain the original EMG data sets on the basis of a linear combination of muscle synergies and their corresponding coefficients, the modulation of the EMGs from supra-brainstem or supra-medullary circuitries can be reflected in the coefficients of the muscle synergies.

Based on the findings of the thesis, I speculate that neural elements underlying a set of muscle synergies required for one form of movements (e.g., jumps) may be shared with neural elements underlying a set of muscle synergies required for another form of movements (e.g., kicks). Therefore, the shared circuitry may be part of a multitask processor

involved in the generation of each multiple motor task (Stein and Smith, 1997). In addition, the shared synergies, the synergies utilized in execution of all four natural movements, may potentially implement a biomechanical or kinematic function that is critical in the construction of several motor behaviors (Cheung, 2007).

Motor primitives or muscle synergies extracted by a range of algorithms or assumed in various muscle models

In the literature on modular organization of movements, motor and movement primitives and modules have been defined at several different levels including the behavioral, neural, and muscle levels with complicated mapping among the elementary building blocks (Flash and Hochner, 2005). A number of computational methods have been used to extract primitives: these include principal component analysis (PCA), probabilistic PCA, hidden Markov models, factor analysis (FA), non-negative matrix factorization (NMF),and independent component analysis (ICA).

One may, therefore, question whether motor modules can be defined differently when a range of different computational algorithms are applied to extract the primitives. Tresch et al. (2006) applied different algorithms to identical data sets in order to compare the resulting motor primitives. The results showed that most of the algorithms used to identify muscle synergies perform comparably. Specifically, the NMF, ICA, and FA algorithms performed similarly on non-negative, simulated data sets. In addition, when these methods were applied to experimentally obtained data sets, the best performing algorithms (NMF, ICA, FA, ICA applied to the subspace defined by PCA, and a version of probabilistic ICA with non-negativity constraints) identified synergies very similar to one another. Thus, the overall results suggest that the synergies extracted by NMF in this thesis may not be an artifact of NMF. The muscle synergies found in the thesis may reflect basic aspects of muscle activation patterns underlying the four major types of motor behaviors.

Another potential question can be raised about the assumed muscle model. In this thesis, the muscle model assumes that the muscle synergy is defined as a balance of amplitude of muscle activations and that the corresponding coefficient has temporal information of muscle activation recorded during movements. The time-invariant synergies demonstrate an invariant spatial organization of the muscle patterns (d'Avella and Bizzi, 2003). In contrast, the muscle activation pattern can be modeled as a combination of time-varying synergies that

capture fixed relationships of muscle activation in both the spatial and time domains (d'Avella and Tresch, 2002; d'Avella et al., 2003; d'Avella et al., 2006). The reasons that this thesis adopted the time-invariant muscle synergy model were as follows. First, it is difficult to entail the increase in the duration of muscle activation of motor behaviors (especially medullary motor behaviors) recorded after the transection, because the duration of a single time-varying muscle synergy should be set constant in the current time-varying synergy model. Second, in terms of their spatial structure, given by the synergy activations averaged across time, the time-varying synergies closely matched the synchronous synergies (d'Avella and Bizzi, 2005). The time-invariant synergy model is sufficient to understand the spatial structure of muscle activation underlying motor behaviors I observed in this thesis. Third, as shown in d'Avella and Bizzi (2005), the R^2 value for the reconstruction of each data set by combinations of the identical number of time-invariant synergies was greater than the R^2 value for the reconstruction of the identical data set by combinations of the identical number of time-varying synergies. The result is reasonable considering that the number of parameters in the time-invariant synergy model was greater than the number in the time-varying synergy model.

In summary, the goal of this thesis has been to test the hypothesis that localized neural divisions of the central nervous system structure and combine muscle synergies, or motor primitives, in order to execute natural movements. To test the given hypothesis, two different sets of experiments, each with two substages of EMG recording sessions at different times, were designed and performed. The first set of experiment tested whether the neural circuits within the brainstem and spinal cord were involved in structuring and combining muscle synergies underlying natural movements. The second set of experiments tested whether the entire repertoire of muscle synergies underlying the four major types of natural movements is structured by the neural circuitries of the medulla and spinal cord.

EMG analysis found the main results to be as follows. First, the non-negative matrix factorization was applied to data sets recorded from intact and reduced preparations and confirmed the low and comparable dimensionalities of the data sets. Four to six synergies can explain >90% of the total variance of the EMG data for all natural movements and "brainstem" movements, while six to seven synergies account for the same amount of variability in the dataset recorded from the "medullary" preparations. Second, there exist two

different types of synergies: (1) synergies common to both natural movements in intact animals and behaviors generated by the reduced preparations (i.e., brainstem or medullary animal preparations), and (2) synergies specific to individual motor behaviors. Three, when the transection was at the level of rostral midbrain, all types of natural movements observed in intact animals could be evoked. Four, when the transection was at the level of rostral medulla, a partial repertoire of natural movements whose sequence is similar to that of natural movements could be performed by the frogs. Five, almost all synergies utilized in the execution of natural motor behaviors remain invariant after transection at the level of the caudal end of the third ventricle or at the level of the caudal end of the pons.

Overall, the major findings of the given study suggest the following conclusions about how the neural divisions in motor coordination and movement execution are functionally differentiated: (1) the neural network within the brainstem and spinal cord are necessary and sufficient in combining muscle synergies in the organization of natural movements, and (2) the modulation of muscle synergies underlying natural movements from the supra-medullary circuitries is minor, so the neural circuitries within the medulla and spinal cord are sufficient to structure the repertoire of muscle synergies in the execution of natural motor behaviors.

References

Averbeck BB, Chafee MV, Crowe DA, Georgopoulos AP (2002) Parallel processing of serial movements in prefrontal cortex. Proc Natl Acad Sci USA 99:13172-13177.
Barale F, Corvaja N, Pompeiano O (1971) Vestibular influences on postural activity in frog. Arch Ital Biol 109:27-36.
Bernstein N (1967) The coordination and regulation of movements. New York: Pergamon Press.
Bizzi E, Cheung VCK, d'Avella A, Saltiel P, Tresch M (2008) Combining modules for movement. Brain Res Rev 57(1):125-33.
Bizzi E, Giszter SF, Loeb E, Mussa-Ivaldi F, Saltiel P (1995) Modular organization of motor behavior in the frog's spinal cord. Trends Neurosci 18:442–446.
Bizzi E, Mussa-Ivaldi FA, Giszter SF (1991) Computations underlying the execution of movement: a biological perspective. Science 253:287-291.
Bizzi E, Tresch MC, Saltiel P, d'Avella A (2000) New perspectives on spinal motor systems. Nat Rev Neurosci 1:101–108.
Boothby KM, Roberts A (1992a) The stopping response of Xenopus laevis embryos: behaviour, development and physiology. J Comp Physiol A 170:171-180.
Boothby KM, Roberts A (1992b) The stopping response of Xenopus laevis embryos: pharmacology and intracellular physiology of rhythmic spinal neurons and hindbrain neurons. J Exp Biol 169:65-86.
Bregman BS, Cruce WLR (1980) Normal dendritic morphology of frog spinal motoneurons. A Golgi study. J Comp Neurol 193:1035-1045.
Brown TG (1911) The intrinsic factors in the act of progression in the mammal. Proc R Soc Lond B Biol Sci 84:308-319.
Cappellini G, Ivanenko YP, Poppele RE, Lacquaniti F (2006) Motor patterns in human walking and running. J Neurophysiol 95:3426-3437.
Cheng J, Stein RB, Jovanovic K, Yoshida K, Bennett DJ, Han Y (1998) Identification, localization, and modulation of neural networks for walking in the mudpuppy (Necturus maculatus) spinal cord. J Neurosci 18:4295–4304.
Cheung VCK (2007) Sensory modulation of muscle synergies for motor adaptation during natural behaviors. Ph.D. thesis, Massachusetts Institute of Technology.
Cheung VC, d'Avella A, Tresch MC, Bizzi E (2005) Central and sensory contributions to the activation and organization of muscle synergies during natural motor behaviors. J Neurosci 25(27):6419-34.
Clarac F (1991) How do sensory and motor signals interact during locomotion? In: Motor control: concepts and issues (Humphrey DR, Freund H-J, eds), pp 199-221. New York: Wiley.
Cruce WLR (1974a) The anatomical organization of hindlimb motoneurons in the lumbar spinal cord of the frog, Rana catesbeiana. J Comp Neurol 153:59-76.
Cruce WLR (1974b) A supraspinal monosynaptic input to hindlimb motoneurons in lumbar spinal cord of the frog, Rana catesbeiana. J Neurophysiol 37:691-704.
d'Avella A, Saltiel P, Bizzi E (2003) Combinations of muscle synergies in the construction of a natural motor behavior. Nat Neurosci 6(3):300-308.
d'Avella A, Bizzi E (2005) Shared and specific muscle synergies in natural motor behaviors. Proc Natl Acad Sci USA 102:3076-3081.
d'Avella A, Portone A, Fernandez L, Lacquaniti F (2006) Control of fast-reaching movements by muscle synergy combinations. J Neurosci 26(30):7791-7810.
d'Avella A, Tresch MC (2002) Modularity in the motor system: decomposition of muscle patterns as combinations of time-varying synergies. In: Advances in neural information

processing, vol. 14 (Dietterich TG, Becker S, Ghahramani Z, ed.), pp 141-148. Cambridge, MA: MIT Press.
Ebbesson SOE (1969) Brain stem afferents from the spinal cord in a sample of reptilian and amphibian species. Ann NY Acad Sci 167:80-101.
Ebbesson SOE (1976) Morphology of the spinal cord. In: Llinas R, Precht W (eds) Frog neurobiology. Springer, Berlin Heidelberg New York, pp 679-706.
Engberg I, Lundberg A (1969) An electromyographic analysis of muscular activity in the hindlimb of the cat during unrestrained locomotion. Acta Physiol Scand 75:614-630.
Erulkar SD, Soller RW (1980) Interactions among lumbar motoneurons on opposite sides of the frog spinal cord: morphological and electrophysiological studies. J Comp Neurol 192:473-488.
Fetz EE, Perlmutter SI, Prut Y (2000) Functions of mammalian spinal interneurons during movement. Curr Opi Neurobiol 10:699-707.
Fishbach A, Roy SA, Bastianen C, Miller LE, Houk JC (2005) Kinematic properties of on line error corrections in the monkey. Exp Brain Res 164:442-457.
Flash T, Hochner B (2005) Motor primitives in vertebrates and invertebrates. Curr Opi Neurobiol 15:660-666.
Full RJ, Koditschek DE (1999) Templates and anchors: neuromechanical hypotheses of legged locomotion on land. J Exp Biol 202:3325-3332.
Fuller PM (1974) Projections of the vestibular nuclear complex in the bullfrog (Rana catesbeiana). Brain Behav Evol 10:157-169.
Giszter SF, Mussa-Ivaldi FA, Bizzi E (1993) Convergent force fields organized in the frog's spinal cord. J Neurosci 13:467-491.
Giszter SF, Kargo WJ (2000) Conserved temporal dynamics and vector superposition of primitives in frog wiping reflexes during spontaneous extensor deletions. Neurocomputing 32-33:775-783.
Golub GH, Van Loan CF (1983) Matrix computations. Baltimore, MD: Johns Hopkins UP.
Gonzalez IC (2003) Linear control model of the spinal processing of descending neural signals. Masters degree thesis, Massachusetts Institute of Technology.
Gottlieb GL (1996) On the voluntary movement of compliant (inertial-viscoelastic) loads by parcellated control mechanisms. J Neurophysiol 76(5):3207-3229.
Greene PH (1972) Problems of organization of motor systems. In: Progress in theoretical biology, vol. 2 (Rosen R, Snell FM, eds), pp 303-338. New York: Academic Press.
Grillner S (1981) Control of locomotion in bipeds, tetrapods, and fish. In: Handbook of physiology, Sect I. The Nervous System (Brooks VB, eds), pp 1179-1236. Bethesda, MD: American Physiological Society.
Grillner S, Deliagina T, Ekeberg O, el Manira A, Hill RH, Lansner A, Orlovsky GN, Wallen P (1995) Neural networks that co-ordinate locomotion and body orientation in lamprey. Trends Neurosci 18:270-279.
Happee R (1993) Goal-directed arm movements. III: Feedback and adaptation in response to inertial perturbations. J Electromyography Kinesiology 3(2):112-122.
Hart CB, Giszter SF (2004) Modular premotor drives and unit bursts as primitives for frog motor behaviors. J Neurosci 24:5269-5282.
Hoffman DS, Strick PL (1993) Step-tracking movements of the wrist. III. Influence of changes in load on patterns of muscle activity. J Neurosci 13(12):5212-5227.
Hulshof JBE, de Boer-van Huizen R, ten Donkelaar HJ (1987) The distribution of motoneurons supplying hind limb muscles in the clawed toad, Xenopus laevis. Acta Morphol Neerl-Scand 25:1-16.

Ivanenko YP, Cappellini G, Dominici N, Poppele RE, Lacquaniti F (2007) Modular control of limb movements during human locomotion. J Neurosci 27(41):11149-61.
Jankowska E, Jukes MG, Lund S, Lundberg A (1967a) The effect of DOPA on the spinal cord. 5. Reciprocal organization of pathways transmitting excitatory action to alpha motoneurones of flexors and extensors. Acta physiol Scand 70:369-388.
Jankowska E, Jukes MG, Lund S, Lundberg A (1967a) The effect of DOPA on the spinal cord. 6. Half-centre organization of interneurones transmitting effects from the flexor reflex afferents. Acta Physiol Scand 70:389-402.
Jing J, Cropper EC, Hurwitz I, Weiss KR (2004) The construction of movement with behavior-specific and behavior-independent modules. J Neurosci 24(28):6315-25.
Kargo WJ, Giszter SF (2000a) Afferent roles in hindlimb wipe-reflex trajectories: free-limb kinematics and motor patterns. J Neurophysiol 83:1480-1501.
Kargo WJ, Giszter SF (2000b) Rapid correction of aimed movements by summation of force-field primitives. J Neurosci 20:409-426.
Kargo WJ, Rome LC (2002) Functional morphology of proximal hindlimb muscles in the frog Rana pipiens. J Exp Biol 205:1987-2004.
Kiehn O (2006) Locomotor circuits in the mammalian spinal cord. Annu Rev Neurosci 29:279-306.
Krishnamoorthy V, Goodman S, Zatsiorsky V, Latash ML (2003) Muscle synergies during shifts of the center of pressure by standing persons: identification of muscle modes. Biol Cybern 89:152-161.
Krouchev N, Kalaska JF, Drew T (2006) Sequential activation of muscle synergies during locomotion in the intact cat as revealed by cluster analysis and direct decomposition. J Neurophysiol 96:1991-2010.
Kugler PN, Kelso JAS, Turvey MT (1980) On the concept of coordinative structures as dissipative structures: I. Theoretical lines of convergence. In: Tutorials in motor behavior (Stelmach GE, Requin J, eds), pp 3-47. Amsterdam:North-Holland.
Lee DD, Seung HS (1999) Learning the parts of objects by non-negative matrix factorization. Nature 401:788-791.
Lee DD, Seung HS (2001) Algorithms for non-negative matrix factorization. In: Advances in neural information processing systems, Vol 13 (Leen TK, Dietterich TG, Tresp V, eds), pp 556-562. Cambridge, MA: MIT.
Lee WA (1984) Neuromuscular synergies as a basis for coordinated intentional action. J Motor Behav 16(2):135-170.
Lockhart DB, Ting LH (2007) Optimal sensorimotor transformations for balance. Nat Neurosci 10(10):1329-36.
Loeb GE (1993) The distal hindlimb musculature of the cat: interanimal variability of locomotor activity and cutaneous reflexes. Exp Brain Res 96:125-140.
Loeb EP, Giszter SF, Saltiel P, Bizzi E, Mussa-Ivaldi FA. (2000) Output units of motor behavior: an experimental and modeling study. J Cogn Neurosci 12(1):78-97.
Lutterotti M (1934) Kleinhirnextirpation bei Hyla arborea. Z Wiss Zool 145:66-78.
Mackey DC, Meichenbaum DP, Shemmell J, Riek S, Carson RG (2002) Neural compensation for compliant loads during rhythmic movement. Exp Brain Res 142: 409-417.
Macpherson JM (1991) How flexible are muscle synergies? In: Motor control: concepts and issues (Humphrey DR, Freund H-J, eds), pp 33-47. New York: John Wiley & Sons.
Magherini PC, Precht W, Richter A (1974) Vestibulospinal effects on hindlimb motoneurons of the frog. Pflugers Arch 348:211-223.
Mardia KV, Kent JT, Bibby JM (1979) In: Multivariate analysis London: Academic.

McClellan AD (1986) Command systems for initiating locomotion in fish and amphibians: parallels to initiation systems in mammals. In: Neurobiology of vertebrate locomotion (Grillner S, Stein PSG, Stuart DG, Forssberg H, Herman RM, eds), pp 3-20. London: MacMillan.
McCrea DA (2001) Spinal circuitry of sensorimotor control of locomotion. J Physiol (Lond) 533.1:41-50.
McKay JL, Ting LH (2008) Functional muscle synergies constrain force production during postural tasks. J Biomech. 41(2):299-306.
Miller LE (2004) Limb Movement: Getting a Handle on Grasp. Curr Biol 14:714-715.
Mortin LI, Keifer J, Stein PSG (1985) Three forms of the scratch reflex in the spinal turtle: movement analyses. J Neurophysiol 53:1501-1516.
Munoz A, Munoz M, Gonzalez A, ten Donkelaar HJ (1996) Evidence for an anuran homologue of the mammalian spinocervicothalamic system: an in vitro tract-tracing study in Xenopus laevis. Eur J Neurosci 8:1390-1400.
Mussa-Ivaldi FA (1997) Nonlinear force fields: a distributed system of control primitives for representing and learning movements. In: Proceedings of the 1997 IEEE international symposium on computational intelligence in robotics and automation, pp 84-90. New York: IEEE Press.
Mussa-Ivaldi FA, Bizzi E (2000) Motor learning through the combination of primitives. Phil Trans R Soc London B 355:1755–1769.
Nieuwenhuys R, Opdam P (1976) Structure of the brain stem. In: Frog neurobiology (Llinas R, Precht W, eds), pp 811-855. Berlin Heidelberg New York: Springer-Verlag.
Overduin SA (2006) Neuromuscular modularity and behavioral correlates of motor control. PhD thesis, Massachusetts Institute of Technology.
Overduin SA, d'Avella A, Roh J, Bizzi E (2008) Modulation of muscle synergy recruitment in primate grasping. J Neurosci 28(4):880–892.
Pasalar S, Roitman AV, Ebner TJ (2005) Effects of speeds and force fields on submovements during circular manual tracking in humans. Exp Brain Res 163:214-225.
Pearson KG, Rossignol S (1991) Fictive motor patterns in chronic spinal cats. J Neurophysiol 66:1874–1887.
Poggio T, Bizzi E (2004) Generalization in vision and motor control. Nature 431(7010):768-774.
Prochazka A (1996) Proprioceptive feedback and movement regulation. In: Handbook of physiology, Sec 12 (Rowell LB, Shepherd JT, eds), pp 89-127. New York: Oxford UP.
Roberts A, Blight AR (1975) Anatomy, physiology and behavioural role of sensory nerve endings in the cement gland of embryonic Xenopus. Proc Roy Soc Lond (Biol) 192:111-127.
Robberts A, Soffe SR, Wolf ES, Yoshida M, Zhao FY (1998) Central circuits controlling locomotion in young frog tadpoles. Ann N Y Acad Sci 860:19-34.
Robertson GA, Mortin LI, Keifer J, Stein PSG (1985) Three forms of the scratch reflex in the spinal turtle: central generation of motor patterns. J Neurophysiol 53:1517-1534.
Rohrer B, Fasoli S, Krebs HI, Hughes R, Volpe B, Frontera WR, Stein J, Hogan N (2002) Movement smoothness changes during stroke recovery. J Neurosci 22:8297-8304.
Roitman AV, Massaquoi SG, Takahashi K, Ebner TJ (2004) Kinematic analysis of manual tracking in monkeys: characterization of movement intermittencies during a circular tracking task. J Neurophysiol 91:901-911.
Rosenthal BM, Cruce WLR (1985) The dendritic extent of motoneurons in frog brachial spinal cord: a computer reconstruction of HRP-filled cells. Brain Behav Evol 27:106-114.

Rossignol S (1996) Neural control of stereotypic limb movements. In: Handbook of physiology, Sec 12 (Rowell LB, Shepherd JT, eds), pp 173-216. New York: Oxford UP.
Rubinson K (1968) Projections of the optic tectum of the frog. Brain Behav Evol 1:529-560.
Sabatini AM (2002) Identification of neuromuscular synergies in natural upper-arm movements. Biol Cybern 86:253-262.
Sala y Pons C (1892) E structura de la medulla espinal de los batracios. Trab Lab Invest Biol Univ Barcelona, pp 3-22.
Sanger TD (2002) Decoding neural spike trains: calculating the probability that a spike train and an external signal are related. J Neurophysiol 87:1659-1663.
Saltiel P, Rossignol S (2004) Critical points in the forelimb fictive locomotor cycle and motor coordination: evidence from the effects of tonic proprioceptive perturbations in the cat. J Neurophysiol 92:1329-1341.
Saltiel P, Tresch MC, Bizzi E (1998) Spinal cord modular organization and rhythm generation: an NMDA iontophoretic study in the frog. J Neurophysiol 80:2323-2339.
Saltiel P, Wyler-Duda K, d'Avella A, Tresch MC, Bizzi E (2001) Muscle synergies encoded within the spinal cord: evidence from focal intraspinal NMDA iontophoresis in the frog. J Neurophysiol 85:605-619.
Saltiel P, Wyler-Duda K, d'Avella A, Ajemian RJ, Bizzi E (2005) Localization and connectivity in spinal interneuronal networks: the adduction-caudal extension-flexion rhythm in the frog. J Neurophysiol 94(3):2120-2138.
Schotland JL, Rymer WZ (1993) Wipe and flexion reflexes of the frog. II. Responses to perturbations. J Neurophysiol 69(5):1736-1748.
Schouenborg J (2002) Modular organisation and spinal somatosensory imprinting. Brain Res Brain Res Rev 40(1-3):80-91.
Schouenborg J, Weng HR (1994) Sensorimotor transformation in a spinal motor system. Exp Brain Res 100:170–174.
Schouenborg J, Weng HR, Kalliomäki J, Holmberg H (1995) A survey of spinal dorsal horn neurones encoding the spatial organization of withdrawal reflexes in the rat. Exp Brain Res 106:19–27.
Shapovalov AI (1975) Neuronal organization and synaptic mechanisms of supraspinal motor control in vertebrates. Rev Physiol Biochem Pharmacol 72:1-54.
Sherrington CS (1948) The Integrative Action of the Nervous System. Cambridge Univ. Press, Cambridge, U.K.
Stein PS, Camp AW, Robertson GA, Mortin LI (1986) Blends of rostral and caudal scratch reflex motor patterns elicited by simultaneous stimulation of two sites in the spinal turtle. J Neurosci 6:2259–2266.
Stein PSG, Smith JL (1997) Neural and biomechanical control strategies for different forms of vertebrate hindlimb motor tasks. In: Neurons, networks, and motor behavior (Stein PSG, Grillner S, Selverston AI, Stuart DG, eds), pp 61-73. Cambridge, MA: MIT Press.
Stein PSG, Victor JC, Field EC, Currie SN (1995) Bilateral control of hindlimb scratching in the spinal turtle: contralateral circuitry contributes to the normal ipsilateral motor pattern of fictive rostral scratching. J Neurosci 15:4343-4355.
Szekely G (1976) The morphology of motoneurons and dorsal root fibers in the frog spinal cord. Brain Res 103:275-290.
ten Donkelaar HJ (1982) Organization of descending pathways to the spinal cord in amphibians and reptiles. Prog Brain Res 57:25-67.
ten Donkelaar HJ (1990) Brainstem mechanisms of behavior: comparative aspects. In: Brainstem mechanisms of behavior (Klemm WR, Vertes RP, eds), p 199-237. New York:

Wiley.
ten Donkelaar HJ (1998) Anurans. In: The central nervous system of vertebrates (Nieuwenhuys R, Ten Donkelaar HJ, Nicholson C, eds), pp 1151-1314. New York: Springer.
Thoroughman KA, Shadmehr R (2000) Learning of action through adaptive combination of motor primitives. Nature 407:742-747.
Ting LH, Macpherson JM (2005) A limited set of muscle synergies for force control during a postural task. J Neurophysiol 93:609-613.
Torres-Oviedo G, Macpherson JM, Ting LH (2006) Muscle synergy organization is robust across a variety of postural perturbations. J Neurophysiol 96:1530-1546.
Torres-Oviedo G, Ting LH (2007) Muscle synergies characterizing human postural responses. J Neurophysiol 98:2144–2156.
Tresch MC, Cheung VCK, d'Avella A (2006) Matrix factorization algorithms for the identification of muscle synergies: evaluation on simulated and experimental data sets. J Neurophysiol 95:2199–2212.
Tresch MC, Saltiel P, Bizzi E (1999) The construction of movement by the spinal cord. Nat Neurosci 2:162-167.
Tresch MC, Saltiel P, d'Avella A, Bizzi E (2002) Coordination and localization in spinal motor systems. Brain Res Brain Res Rev 40(1-3):66-79.
Tuller B, Turvey MT, Fitch HL (1982) The Bernstein perspective: II. The concept of muscle linkage or coordinative structure. In: Human motor behavior: an introduction (Kelso JAS, eds), pp 253-270. Hillsdale, NJ: Lawrence Erlbaum Associates.
Viviani P (1986) Do units of motor action really exist? In: Generation and Modulation of Action Patterns (Heuer H, Fromm C, eds), pp 201-216. New York: Springer.
Weiss EJ, Flanders M (2004) Muscular and postural synergies of the human hand. J Neurophysiol 92:523-535.